Supporting Material

Selective Binding and Extraction of Aqueous Dihydrogen Phosphate Solutions via Three-armed Thiourea Receptors

Evgeny V. Beletskiy[1,2] and Steven R. Kass[2]*

[1]Current address: Department of Chemical and Biological Engineering, Northwestern University, 2145 Sheridan Rd., Evanston, IL 60208 USA

[2]Department of Chemistry, University of Minnesota, 207 Pleasant St. S.E., Minneapolis, MN 55455 USA.

*To whom correspondence should be addressed. E-mail: kass@umn.edu

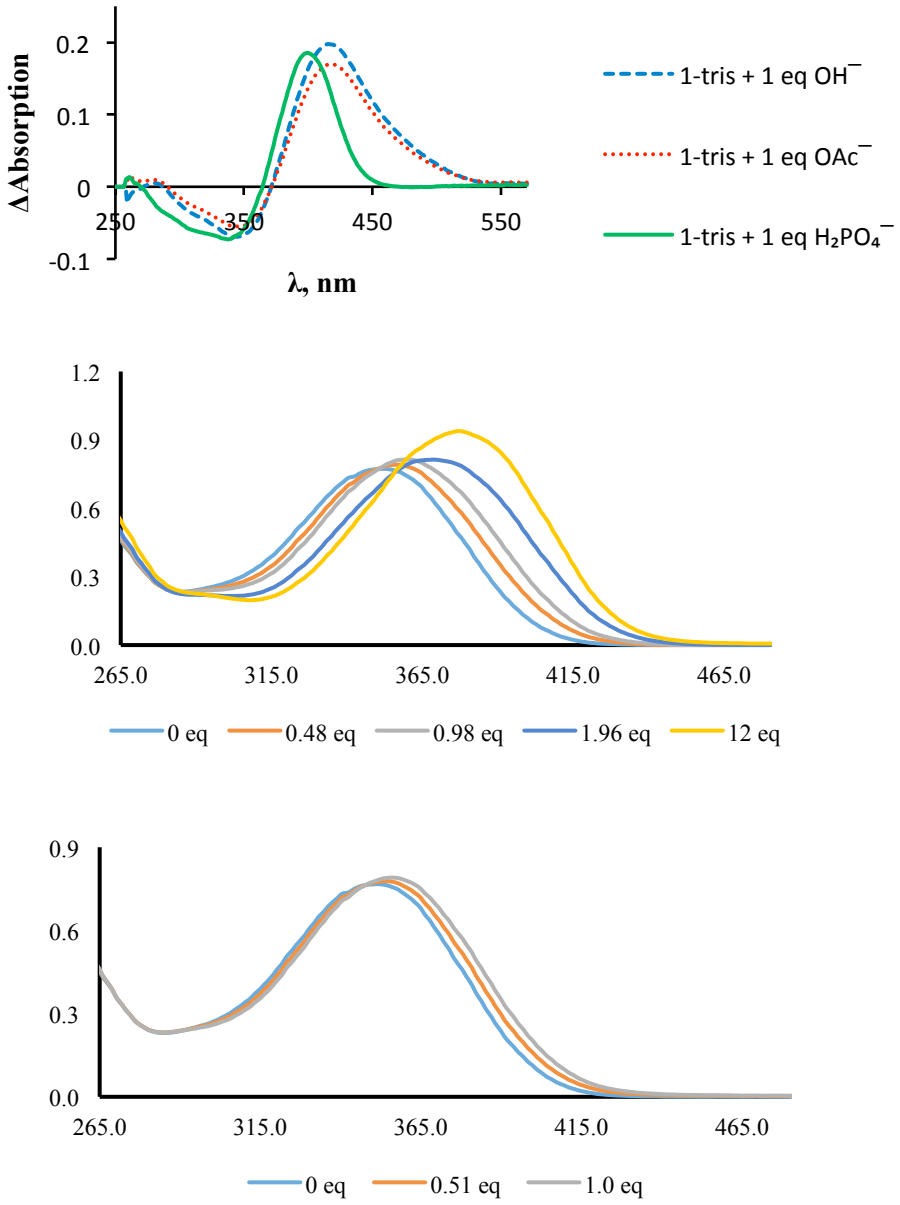

Figure S1. UV-visible absorbance changes upon the addition of 1 equivalent of tetrabutyl-ammonium salts of hydroxide, acetate, and dihydrogen phosphate at room temperature to 15 μM **1-tris** in 0.5% H_2O and 99.5% DMSO (v/v) [top]. Full spectra for the addition of 0, 0.48, 0.98, 1.96 and 12 equivalents of tetrabutyl ammonium dihydrogen phosphate to **1-tris** in 0.5%/99.5% H_2O and DMSO; the isobestic point shifts after 1 equivalent indicative of a new type of interaction [middle]. Representative spectra for the addition of 0, 0.51 and 1.00 equivalents of tetrabutyl ammonium acetate to **1-tris** in H_2O and DMSO (0.5%/99.5) [bottom].

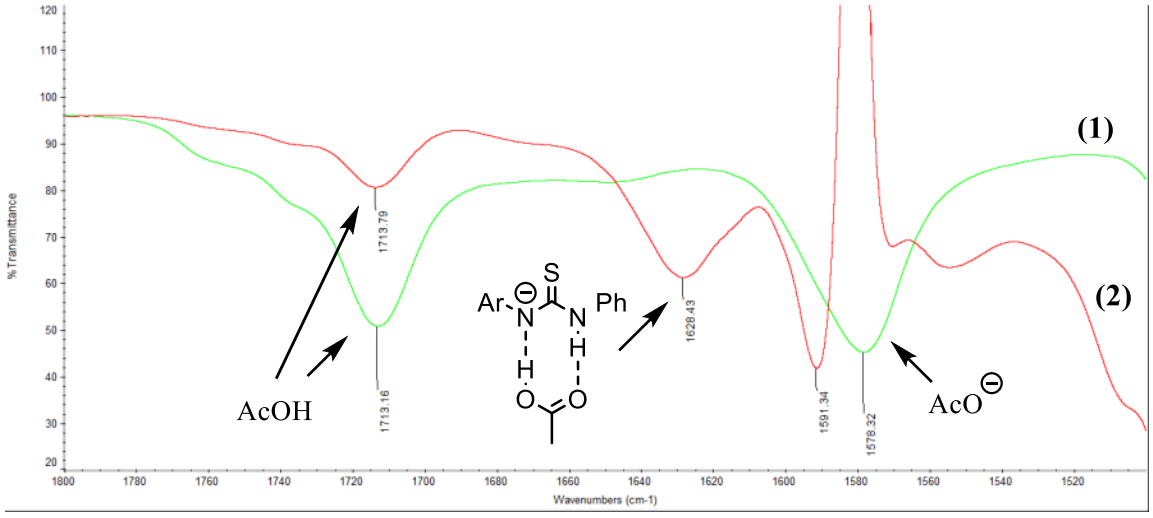

Figure S2. Infrared spectra were recorded in DMSO-d_6 with a 0.1 mm NaCl liquid cell and a Thermo Scientific Nicolette iS5 spectrometer. The results displayed from 1500-1800 cm^{-1} for a 1:1 60 mM solution of HOAc and Bu_4NOAc (**1**) and a **1-mono** (60 mM) and Bu_4NOAc (90 mM) mixture (**2**) were background corrected for the solvent in both cases and tetrabutylammonium acetate in the latter spectrum.

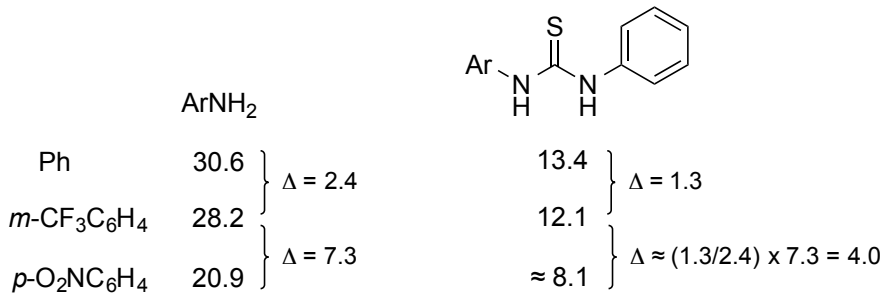

Figure S3. Prediction scheme for the DMSO pK_a of **1-mono – 1-tris** based upon previously measured values[40,41].

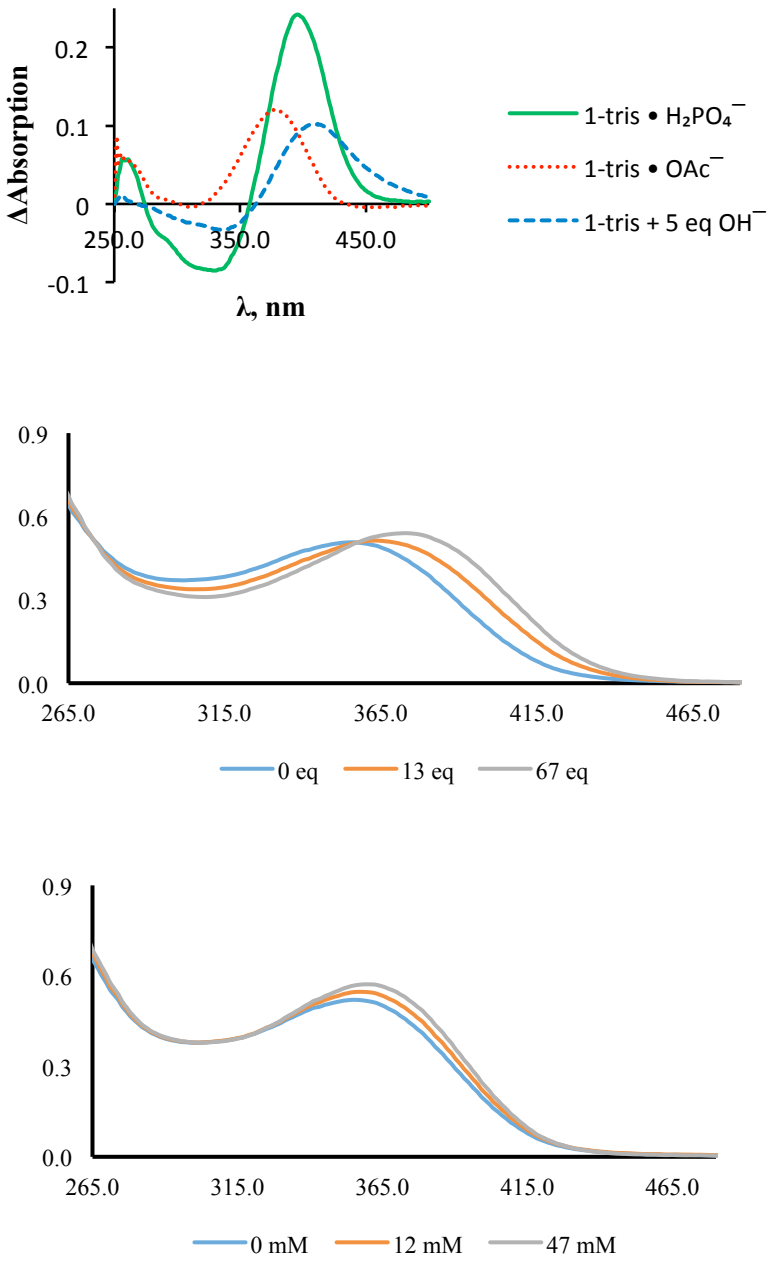

Figure S4. UV-visible absorbance changes upon the addition of 1 equivalent of tetrabutyl-ammonium salts of hydroxide, acetate, and dihydrogen phosphate at room temperature to 15 μM **1-tris** in 25% H_2O and 75% DMSO (v/v) [top]. Representative UV-visible spectra for the addition of 0, 13 and 67 equivalents of tetrabutyl ammonium dihydrogen phosphate to **1-tris** in H_2O/DMSO (25%/75%) [middle]. Sample spectra obtained by adding 0, 12 and 47 mM tetrabutyl ammonium acetate to **1-tris** in 25%/75% H_2O and DMSO [bottom].

Binding of 1-tris with $H_2PO_4^-$ in 0.5% (v/v) aqueous DMSO.

Job's plot. A 100 μM solution of **1-tris** in 0.5% H_2O–DMSO (105 μL) was titrated with 0.5% H_2O–DMSO and a 100 μM solution of tetrabutylammonium dihydrogen phosphate in 0.5% H_2O–DMSO so that the sum of the total concentrations of the two were constant (10.0 μM). UV absorptions at λ = 400 nm are given in Table S1. Since $\Delta A = A - A_0 = A_{SX}$ and ΔA is proportional to [*SX*], the binding stoichiometry is given at the maximum of a plot of ΔA *vs.* anion % in the mixture, where A_0 is the free receptor absorption and A_{SX} is the absorption of the bound species *SX*; A_0 = 0.265 for a 15 μM solution[42]. The maximum was observed at 0.5 indicating that the binding mode is 1:1 (Figure S5).

Binding isotherm. A 15.0 μM solution of **1-tris** in 0.5% H_2O–DMSO (2.00 mL) was titrated with a 1.61 mM (entries 1-12) followed by a 33.9 mM (entries 13-14) solution of tetrabutylammonium dihydrogen phosphate in 0.5% H_2O–DMSO at 23 °C (Table S2). A linear dependence of the absorbance versus the number of equivalents of $H_2PO_4^-$ in the 0.0 - 0.94 range (Figure S6, left) is consistent with complete binding and leads to A_{max} = 0.426. If one assumes that ≥ 89% of the thiourea is bound when 1 equivalent $H_2PO_4^-$ is added, then $K \geq 5 \times 10^6$ M^{-1}. The change in absorption at higher concentrations of $H_2PO_4^-$ was ascribed to deprotonation of the receptor-bound complex by free $H_2PO_4^-$ to afford thiourea-bound HPO_4^{2-}.[43] Non-linear curve fitting of these data affords an apparent binding affinity $K_{11} = 5.2 \times 10^5$ M^{-1} and A_{max} = 0.544 (not shown) or an equilibrium constant K = 3.9 and A_{max} = 0.548 calculated in analogous way for this process (Figure S6, right).

Table S1. Job's plot data for the interaction of **1-tris** with $H_2PO_4^-$ ($\lambda = 400$ nm).

Entry	µL solvent added	µL $H_2PO_4^-$ added	[thiourea]$_0$, µM	[$H_2PO_4^-$]$_0$, µM	Absorption	ΔA
1	1350	45	7.00	3.00	0.2266	0.0741
2	67	7.4	6.67	3.33	0.2268	0.0791
3	158	17.6	6.00	4.00	0.2156	0.0774
4	315	35.0	5.00	5.00	0.2032	0.0794
5	472	52.5	4.00	6.00	0.1804	0.0709
6	475	52.8	3.33	6.67	0.1641	0.0643
7	312	34.7	3.00	7.00	0.1570	0.0618

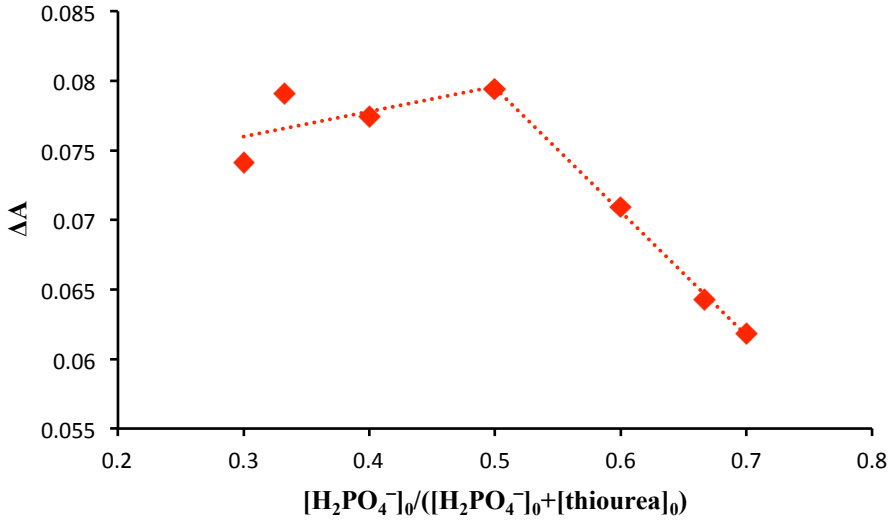

Figure S5. Job's plot for the interaction of **1-tris** with $H_2PO_4^-$.

Table S2. Data for the titration of **1-tris** with $H_2PO_4^-$ in 0.5% H_2O–DMSO at 400 nm.

Entry	μL $H_2PO_4^-$ added	$[thiourea]_0$, μM	$[H_2PO_4^-]_0$, μM	Observed absorption[a]	Calculated absorption[b]
0	0	15.00	0.00	0.2400	0.2421
1	3	14.98	2.41	0.2719	0.2716
2	5	14.96	4.01	0.2916	0.2913
3	7.5	14.94	6.01	0.3175	0.3159
4	10	14.93	8.00	0.3408	0.3405
5	12.5	14.91	9.99	0.3667	0.3651
6	15	14.89	12.0	0.3902	0.3897
7	17.5	14.87	13.9	0.4116	0.4143
8	20	14.85	15.9	0.4341	0.4346
9	25	14.82	19.8	0.4723	0.4631
10	30	14.78	23.8	0.4937	0.4854
11	40	14.71	31.5	0.5108	0.5120
12	50	14.63	39.2	0.5191	0.5243
13	5	14.60	121	0.5385	0.5431
14	10	14.56	203	0.5477	0.5451

[a] Concentration-corrected absorptions. [b] From the linear (entries 0-7) and non-linear (entries 8-14) curve fits.

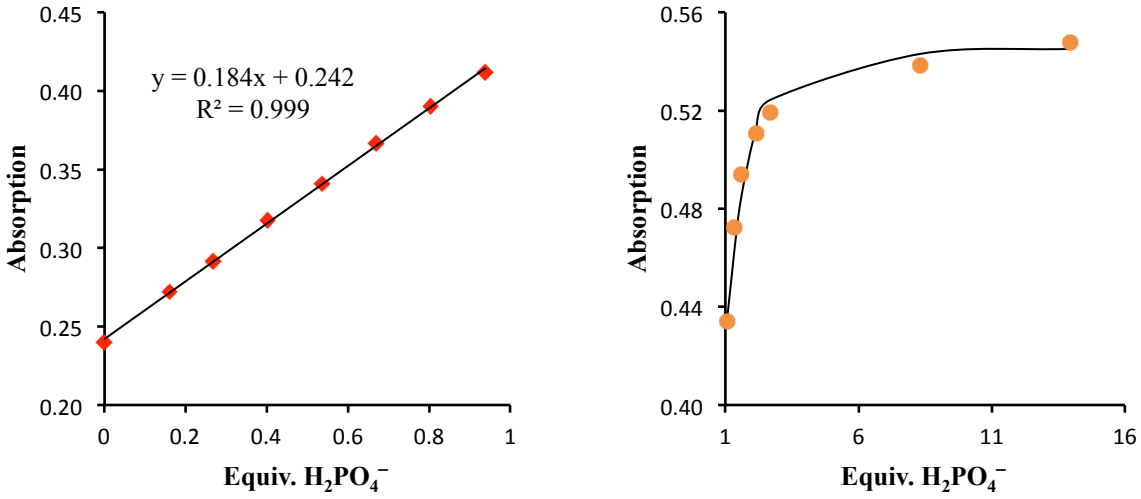

Figure S6. Least-squares fittings of the titration data in Table S2.

Binding of 1-tris with OAc^- in 0.5% (v/v) aqueous DMSO.

Job's plot. A 100 μM solution of **1-tris** in 0.5% H_2O–DMSO (105 μL) was titrated with 0.5% H_2O–DMSO and a 100 μM solution of tetrabutylammonium acetate in 0.5% H_2O–DMSO so that the sum of the total concentrations of the two were constant (10.0 μM). UV absorptions at λ = 416 nm are given in Table S3. Since $\Delta A = A - A_0 = A_{sx}$ and ΔA is proportional to [*SX*], the binding stoichiometry is given at the maximum of a plot of ΔA *vs.* anion % in the mixture, where A_0 is the free receptor absorption and A_{SX} is the absorption of the bound species *SX*; A_0 = 0.102 for a 15 μM solution. The maximum was observed at *ca.* 0.55 indicating that the binding mode is 1:1 and is followed by subsequent 1:2 complex formation (Figure S7).

Titration data. A 15 μM solution of **1-tris** in 0.5% H_2O–DMSO (2.10 mL) was titrated with a 4.31 mM solution of tetrabutylammonium acetate in 0.5% H_2O–DMSO at 24 °C (Table S4). A linear dependence of the absorbance versus the number of equivalents of OAc^- in the 0.0 - 1.00 range (Figure S8) is consistent with irreversible deprotonation. The spectral data is also the same as observed when 1 equivalent of tetrabutylammonium hydroxide is added. A linear least squares fit affords A_{max} = 0.255. The change in absorption at higher concentrations of OAc^- was ascribed to the interaction of the other two thiourea arms and 1:2 complex formation (see Job's plot).

Table S3. Job's plot data for the interaction of **1-tris** with OAc^-.

Entry	μL solvent added	μL OAc^- added	$[thiourea]_0$, μM	$[OAc^-]_0$, μM	Absorption	ΔA
1	1350	45	7.00	3.00	0.1403	0.0159
2	67	7.4	6.67	3.33	0.1391	0.0178
3	158	17.6	6.00	4.00	0.1346	0.0201
4	315	35.0	5.00	5.00	0.1300	0.0255
5	472	52.5	4.00	6.00	0.1198	0.0254
6	475	52.8	3.33	6.67	0.1103	0.0226
7	312	34.7	3.00	7.00	0.1053	0.0212

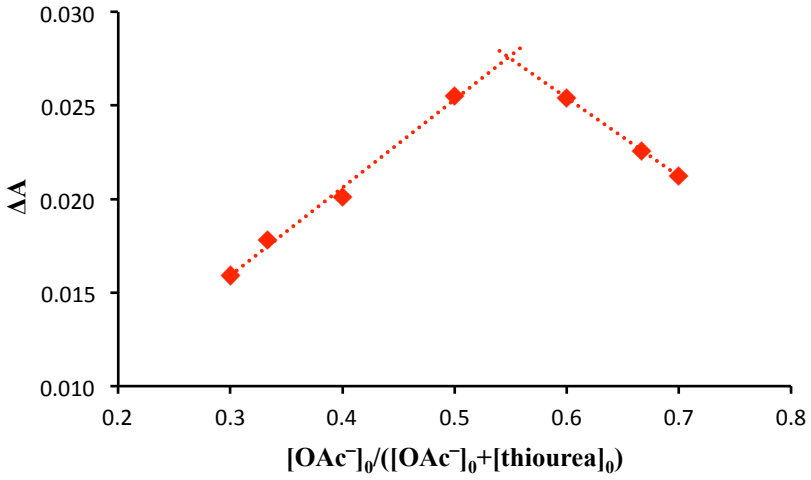

Figure S7. Job's plot for the interaction of **1-tris** with OAc^-.

Table S4. Data for the titration of **1-tris** with OAc^- in 0.5% H_2O–DMSO at 416 nm.

Entry	μL OAc^- added	$[thiourea]_0$, μM	$[OAc^-]_0$, μM	Observed absorption[a]	Calculated absorption[b]
0	0	15.00	0.0	0.0895	0.0894
1	2	14.99	4.3	0.1367	0.1371
2	3	14.98	6.4	0.1599	0.1609
3	4	14.97	8.6	0.1847	0.1847
4	5	14.96	10.7	0.2091	0.2085
5	6	14.96	12.9	0.2323	0.2324
6	7	14.95	15.0	0.2543	0.2562
7	8.5	14.94	18.2	0.2848	
8	10	14.93	21.4	0.3177	
9	12	14.91	25.7	0.3454	
10	14	14.90	29.9	0.3683	
11	16	14.88	34.2	0.3888	
12	18	14.87	38.4	0.4024	
13	21	14.84	44.7	0.4111	
14	25	14.82	53.1	0.4182	
15	30	14.78	63.6	0.4257	

[a] Concentration-corrected absorptions. [b] From the linear fit.

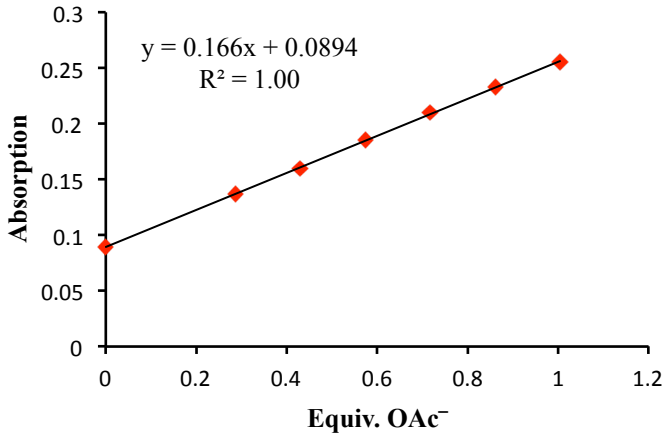

Figure S8. Linear least squares fitting of the titration data in Table S4.

Binding of 1-mono with $H_2PO_4^-$ in 0.5% (v/v) aqueous DMSO. A 14.3 μM solution of **1-mono** in 0.5% H_2O–DMSO (2.10 mL) was titrated with a 30.0 mM solution of tetrabutylammonium dihydrogen phosphate in 0.5% H_2O–DMSO at 23 °C (Table S5). Non-linear curve fitting of the titration data affords $K = 4.0 \times 10^4$ M^{-1} and $A_{max} = 0.205$ (Figure S9).

Binding of 1-mono with OAc^- in 0.5% (v/v) aqueous DMSO. To a 30 μM solution of **1-mono** in 0.5% H_2O–DMSO (2.00 mL) was added a 5.0 mM solution of tetrabutylammonium hydroxide in 0.5% MeOH–DMSO (12.0 μL, 1.00 equiv.) followed by a 5.00 mM acetic acid solution in DMSO (12.0 μL, 1.00 equiv.). Less than a 10% change was observed after addition of the acetic acid indicating that little if any proton transfer takes place from the acid.

Table S5. Data for the titration of **1-mono** with $H_2PO_4^-$ in 0.5% H_2O–DMSO at 454 nm.

Entry	µL $H_2PO_4^-$ added	$[thiourea]_0$, µM	$[H_2PO_4^-]_0$, µM	Observed absorption	Calculated absorption[a]
0	0	14.3	0.0	0.0315	0.0315
1	1	14.3	14.3	0.0835	0.0819
2	2	14.3	28.5	0.1126	0.1129
3	3	14.3	42.8	0.1316	0.1325
4	4	14.3	57.0	0.1451	0.1456
5	5	14.3	71.3	0.1547	0.1548
6	7	14.2	99.7	0.1668	0.1668
7	10	14.2	142	0.1767	0.1767
8	15	14.2	212	0.1866	0.1848
9	20	14.2	283	0.1885	0.1889
10	30	14.1	423	0.1929	0.1926
11	50	14.0	698	0.1936	0.1946

[a] From the non-linear curve fit.

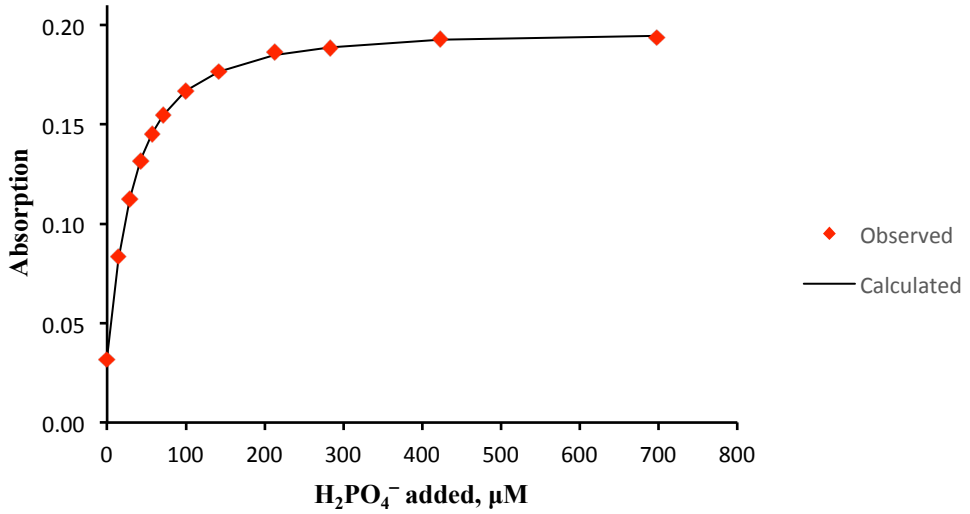

Figure S9. Non-linear least squares fitting of the titration data in Table S5.

Binding of 1-tris with $H_2PO_4^-$ in 5% (v/v) aqueous DMSO. A 15 µM solution of **1-tris** in 5% H_2O–DMSO (2.00 mL) was titrated with a 2.14 mM solution of tetrabutylammonium dihydrogen phosphate in 5% H_2O–DMSO at 24 °C (Table S6). Non-linear curve fitting of the titration data affords $K = 2.3 \times 10^5$ M^{-1} and $A_{max} = 0.549$ (Figure S10).

Table S6. Data for the titration of **1-tris** with $H_2PO_4^-$ in 5% H_2O–DMSO at 399 nm.

Entry	μL $H_2PO_4^-$ added	$[thiourea]_0$, μM	$[H_2PO_4^-]_0$, μM	Observed absorption	Calculated absorption[a]
0	0	15.00	0	0.2619	0.2619
1	1	14.99	1.07	0.2753	0.2774
2	2	14.99	2.13	0.2901	0.2924
3	3.5	14.97	3.73	0.3122	0.3141
4	5	14.96	5.33	0.3282	0.3345
5	7.5	14.94	7.98	0.3573	0.3656
6	10	14.93	10.6	0.3841	0.3925
7	12.5	14.91	13.3	0.4104	0.4152
8	15	14.89	15.9	0.4346	0.4338
9	17.5	14.87	18.5	0.4532	0.4489
10	20	14.85	21.2	0.4691	0.4609
11	25	14.82	26.4	0.4862	0.4781
12	30	14.78	31.6	0.4933	0.4893
13	40	14.71	41.9	0.4996	0.5016
14	50	14.63	52.1	0.5019	0.5075

[a] From the non-linear curve fit.

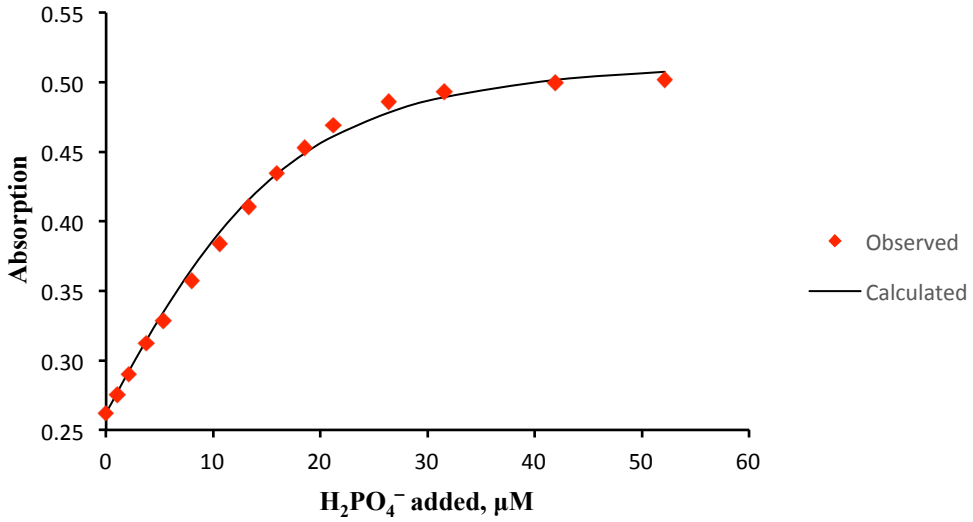

Figure S10. Non-linear least squares fitting of the titration data in Table S6.

Binding of 1-tris with OAc^- in 5% (v/v) aqueous DMSO. A 15 μM solution of **1-tris** in 0.5% H_2O–DMSO (2.10 mL) was titrated with a 4.31 mM solution of tetrabutylammonium acetate in 0.5% H_2O–DMSO at 24 °C (Table S7). A linear dependence of the absorbance versus the number of equivalents of acetate in the 0.0 - 0.93 range (Figure S11) is consistent with irreversible deprotonation and the linear least square fit afforded A_{max} = 0.272. The change in absorption at higher OAc^- concentrations was ascribed to sequential binding or deprotonation (1:2) upon interaction with the remaining two thiourea arms.

Table S7. Data for the titration of **1-tris** with OAc^- in 5% H_2O–DMSO at 411 nm.

Entry	μL OAc^- added	$[thiourea]_0$, μM	$[OAc^-]_0$, μM	Observed absorption[a]	Calculated absorption[b]
0	0	15.00	0.0	0.1314	0.1346
1	2	14.99	4.7	0.1790	0.1772
2	3	14.98	7.0	0.2010	0.1985
3	4	14.97	9.3	0.2215	0.2198
4	5	14.96	11.7	0.2428	0.2411
5	6	14.96	14.0	0.2582	0.2625
6	7	14.95	16.3	0.2749	
7	8.5	14.94	19.8	0.2919	
8	10	14.93	23.2	0.3065	
9	13	14.90	30.2	0.3291	
10	16	14.88	37.1	0.3425	
11	20	14.85	46.3	0.3545	
12	25	14.82	57.7	0.3622	
13	30	14.78	69.1	0.3688	
14	40	14.71	91.6	0.3755	

[a] Concentration-corrected absorptions. [b] From the linear fit.

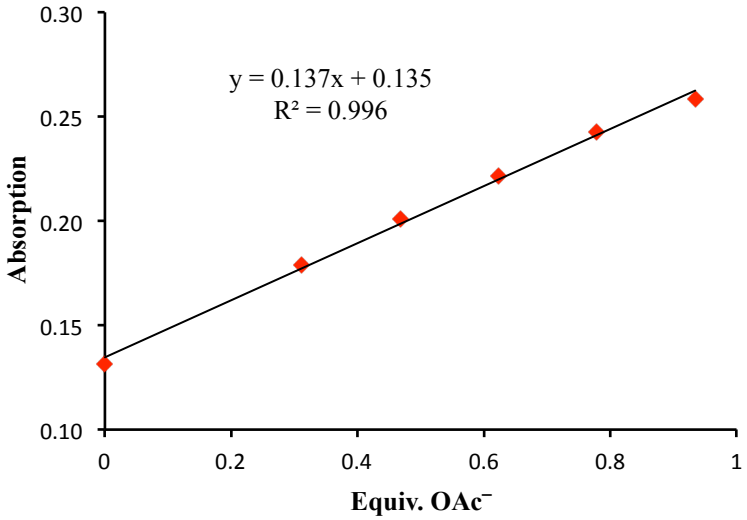

Figure S11. Linear least squares fitting of the titration data in Table S7.

Binding of 1-tris with $H_2PO_4^-$ in 12.5% (v/v) aqueous DMSO. A 15 μM solution of **1-tris** in 12.5% H_2O–DMSO (2.00 mL) was titrated with a 16.1 mM solution of tetrabutylammonium dihydrogen phosphate in 12.5% H_2O–DMSO at 24 °C (Table S8). Non-linear curve fitting of the titration data affords $K = 7.5 \times 10^4$ M^{-1} and $A_{max} = 0.544$ (Figure S12).

Binding of 1-tris with OAc^- in 12.5% (v/v) aqueous DMSO. A 15 μM solution of **1-tris** in 12.5% H_2O–DMSO (2.00 mL) was titrated with a 3.81 mM solution of tetrabutylammonium acetate in 12.5% H_2O–DMSO at 23 °C (Table S9). The wavelength of the maximum change in the concentration-corrected absorption of the thiourea shifted from λ = 413 nm to 406 nm and the titration data was not fit to a binding curve.

Table S8. Data for the titration of **1-tris** with $H_2PO_4^-$ in 12.5% H_2O–DMSO at 397 nm.

Entry	µL $H_2PO_4^-$ added	$[thiourea]_0$, µM	$[H_2PO_4^-]_0$, µM	Observed absorption	Calculated absorption[a]
0	0	15.0	0	0.2608	0.2608
1	1	15.0	8.03	0.3315	0.3298
2	2	15.0	16.1	0.3761	0.3792
3	3	15.0	24.1	0.4086	0.4135
4	4	15.0	32.1	0.4386	0.4374
5	5	15.0	40.1	0.4563	0.4545
6	7.5	14.9	60.1	0.4865	0.4804
7	10	14.9	80.0	0.4968	0.4944
8	15	14.9	119	0.5067	0.5085
9	20	14.9	159	0.5123	0.5150
10	30	14.8	237	0.5162	0.5203
11	130	14.1	981	0.5086	0.5075
12	230	13.5	1658	0.4880	0.4862

[a] From the non-linear curve fit.

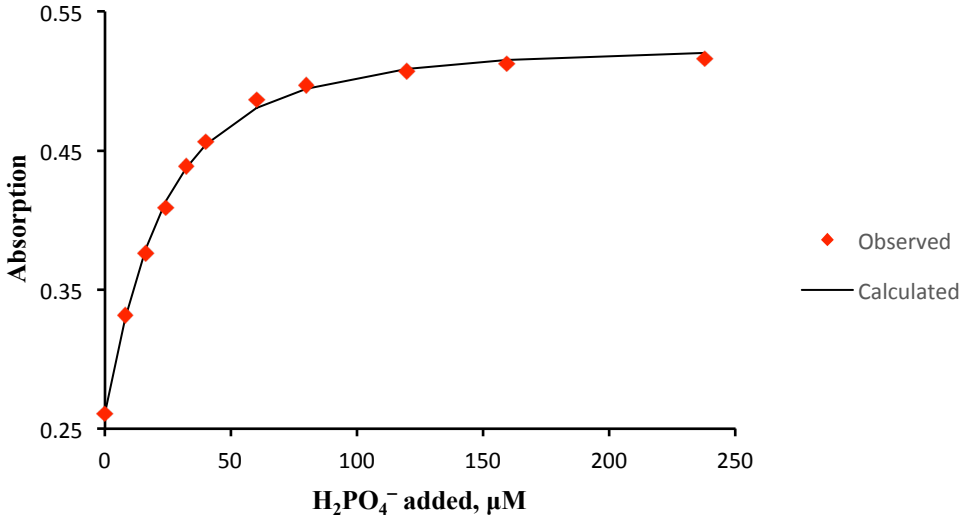

Figure S12. Non-linear least squares fitting of the titration data in Table S8.

Table S9. Data for the titration of **1-tris** with OAc^- in 12.5% H_2O–DMSO at 413 nm.

Entry	μL OAc^- added	$[thiourea]_0$, μM	$[OAc^-]_0$, μM	Observed absorption
0	0	15.00	0.1153	0.1153
1	2	14.99	0.1362	0.1362
2	3.5	14.97	0.1490	0.1490
3	5	14.96	0.1579	0.1579
4	6.5	14.95	0.1667	0.1667
5	8	14.94	0.1726	0.1726
6	10	14.93	0.1791	0.1791
7	15	14.89	0.1900	0.1900
8	20	14.85	0.1985	0.1985
9	30	14.78	0.2070	0.2070
10	40	14.71	0.2111	0.2111
11	60	14.56	0.2148	0.2148
12	80	14.42	0.2143	0.2143

Binding of 1-tris with $H_2PO_4^-$ in 20% (v/v) aqueous DMSO. A 15 μM solution of **1-tris** in 20% H_2O–DMSO (2.00 mL) was titrated with a 16.1 mM solution of tetrabutylammonium dihydrogen phosphate in 20% H_2O–DMSO at 24 °C (Table S10). Non-linear curve fitting of the titration data affords $K = 1.5 \times 10^4$ M^{-1} and $A_{max} = 0.465$ (Figure S13).

Table S10. Data for the titration of **1-tris** with $H_2PO_4^-$ in 20% H_2O–DMSO at 397 nm.

Entry	µL $H_2PO_4^-$ added	$[thiourea]_0$, µM	$[H_2PO_4^-]_0$, µM	Observed absorption	Calculated absorption[a]
0	0	15.00	0	0.2468	0.2468
1	1	14.99	7.73	0.2712	0.2662
2	2	14.99	15.5	0.2874	0.2829
3	3.5	14.97	27.0	0.3080	0.3036
4	5	14.96	38.6	0.3216	0.3204
5	7.5	14.94	57.8	0.3412	0.3419
6	10	14.93	77.0	0.3559	0.3578
7	12.5	14.91	96.1	0.3676	0.3700
8	15	14.89	115	0.3755	0.3795
9	20	14.85	153	0.3923	0.3932
10	25	14.82	191	0.4019	0.4024
11	30	14.78	229	0.4096	0.4090
12	40	14.71	303	0.4176	0.4172
13	50	14.63	377	0.4228	0.4218
14	70	14.49	523	0.4269	0.4258
15	90	14.35	666	0.4273	0.4265

[a] From the non-linear curve fit.

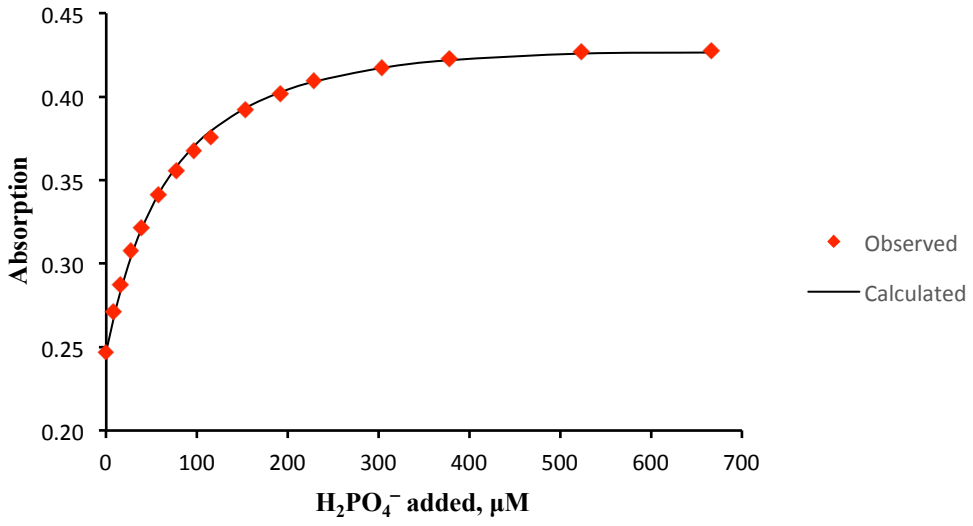

Figure S13. Non-linear least squares fitting of the titration data in Table S10.

Binding of 1-tris with OAc^- in 20% (v/v) aqueous DMSO. A 15 μM solution of **1-tris** in 20% H_2O–DMSO (2.00 mL) was titrated with a 219 mM solution of tetrabutylammonium acetate in 20% H_2O–DMSO containing 15 μM of **1-tris** at 22 °C (Table S11). The wavelength of the maximum change in the concentration-corrected absorption of the thiourea shifted from λ = 406 nm to 384 nm and the titration data could not be fit to a 1:1 binding curve.

Table S11. Data for the titration of **1-tris** with OAc^- in 20% H_2O–DMSO at 384 nm.

Entry	μL OAc^- added	$[thiourea]_0$, mM	$[OAc^-]_0$, mM	Observed absorption
0	0	0.0150	0	0.4171
1	1	0.0150	0.11	0.4269
2	2	0.0150	0.22	0.4284
3	3	0.0150	0.33	0.4293
4	5	0.0150	0.55	0.4302
5	10	0.0149	1.09	0.4340
6	20	0.0149	2.17	0.4443
7	40	0.0147	4.29	0.4517
8	60	0.0146	6.37	0.4579
9	100	0.0143	10.41	0.4663
10	150	0.0140	15.26	0.4731
11	200	0.0136	19.88	0.4806
12	300	0.0130	28.53	0.4903
13	400	0.0125	36.45	0.4959
14	600	0.0115	50.48	0.5072
15	760	0.0109	60.24	0.5119

Binding of 1-tris with $H_2PO_4^-$ in 25% (v/v) aqueous DMSO. A 15 μM solution of **1-tris** in 25% H_2O–DMSO (2.00 mL) was titrated with a 40.0 mM solution of tetrabutylammonium dihydrogen phosphate in 25% H_2O–DMSO at 24 °C (Table S12). Non-linear curve fitting of the titration data affords $K = 4000\ M^{-1}$ and $A_{max} = 0.477$ (Figure S14).

Table S12. Data for the titration of **1-tris** with $H_2PO_4^-$ in 25% H_2O–DMSO at 395 nm.

Entry	µL $H_2PO_4^-$ added	$[thiourea]_0$, µM	$[H_2PO_4^-]_0$, µM	Observed absorption	Calculated absorption[a]
0	0	15	0	0.2398	0.2398
1	2.5	14.98	49.8	0.2807	0.2774
2	5	14.96	99.6	0.3056	0.3048
3	7.5	14.94	149	0.3244	0.3254
4	10	14.92	199	0.3408	0.3414
5	12.5	14.91	248	0.3528	0.3542
6	15	14.89	297	0.3647	0.3646
7	20	14.85	395	0.3804	0.3802
8	25	14.82	493	0.3919	0.3914
9	30	14.78	590	0.3993	0.3997
10	40	14.71	783	0.4110	0.4109
11	50	14.63	974	0.4182	0.4177

[a] From the non-linear curve fit.

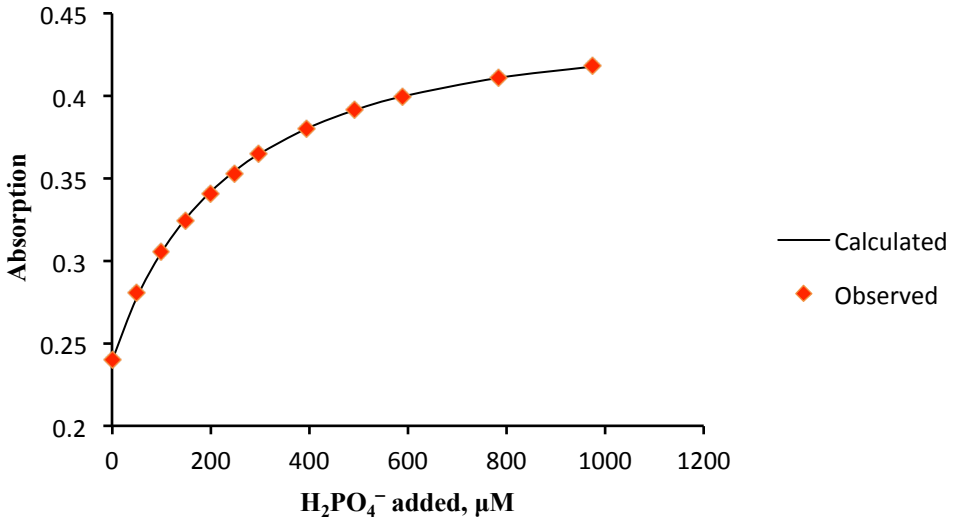

Figure S14. Non-linear least squares fitting of the titration data in Table S12.

Binding of 1-tris with OAc^- in 25% (v/v) aqueous DMSO. A 15 μM solution of **1-tris** in 25% H_2O–DMSO (2.00 mL) was titrated with a 0.513 M solution of tetrabutylammonium acetate in 25% H_2O–DMSO at 24 °C (Table S13). A linear least squares fit in the single-reciprocal plot affords K = 35 M^{-1} and ΔA_{max} = 0.120 (Figure S15, entries 1–14, 8-62% bound (i.e., $\Delta A/\Delta A_{max}$); deviation was observed thereafter presumably due to sequential 1:2 binding).

Table S13. Data for the titration of **1-tris** with OAc^- in 25% H_2O–DMSO at 379 nm.

Entry	μL OAc^- added	$[OAc^-]_0$, M	Observed absorption	ΔA_{cor}	$\Delta A_{cor}/[OAc^-]_0$
0	0	0	0.4075	–	–
1	10	0.00255	0.4153	0.0099	3.873
2	15	0.00381	0.4182	0.0139	3.641
3	20	0.00507	0.4213	0.0180	3.542
4	25	0.00632	0.4236	0.0213	3.376
5	30	0.00757	0.4264	0.0253	3.343
6	35	0.00881	0.4283	0.0283	3.213
7	40	0.01004	0.4299	0.0310	3.083
8	50	0.01249	0.4341	0.0375	2.999
9	60	0.01492	0.4349	0.0404	2.708
10	80	0.01970	0.4394	0.0495	2.511
11	100	0.02439	0.4408	0.0553	2.267
12	125	0.03013	0.4412	0.0612	2.031
13	150	0.03574	0.4401	0.0656	1.835
14	200	0.04657	0.4381	0.0744	1.597
15	300	0.06683	0.4315	0.0887	1.327
16	400	0.08539	0.4207	0.0972	1.138

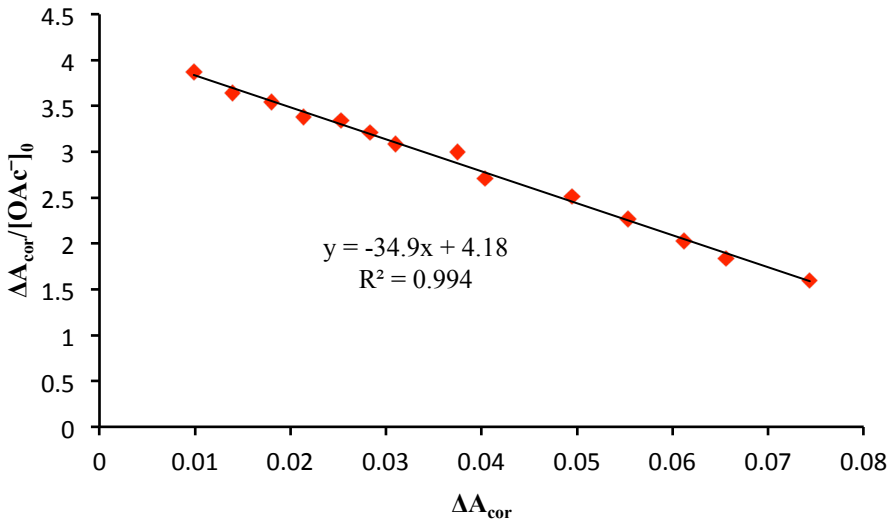

Figure S15. Linear least squares fitting of the titration data in Table S13.

Binding of 1-tris with Cl^- in 25% (v/v) aqueous DMSO. A 15 μM solution of **1-tris** in 25% H_2O–DMSO (2.00 mL) was titrated with solid tetrabutylammonium chloride at 24 °C (Table S14). The volume change was calculated based on the density of TBACl (i.e., 0.98 g/mL). A linear least squares fit of the single-reciprocal plot affords K = 1.5 M^{-1} and ΔA_{max} = 0.298 (Figure S16, 12-66% bound (i.e., $\Delta A/\Delta A_{max}$)).

Table S14. Data for the titration of **1-tris** with Cl^- in 25% H_2O–DMSO at 363 nm.

Entry	mg TBACl added	$[Cl^-]_0$, M	Observed absorption	ΔA_{cor}	$\Delta A_{cor}/[Cl^-]_0$
0	0	0	0.5324	–	–
1	50.7	0.0888	0.5550	0.0369	0.4153
2	103.7	0.1770	0.5662	0.0637	0.3598
3	193.7	0.3167	0.5706	0.0945	0.2985
4	362.7	0.5500	0.5629	0.1345	0.2445
5	632.4	0.8593	0.5311	0.1698	0.1976
6	966.4	1.163	0.4879	0.1956	0.1681

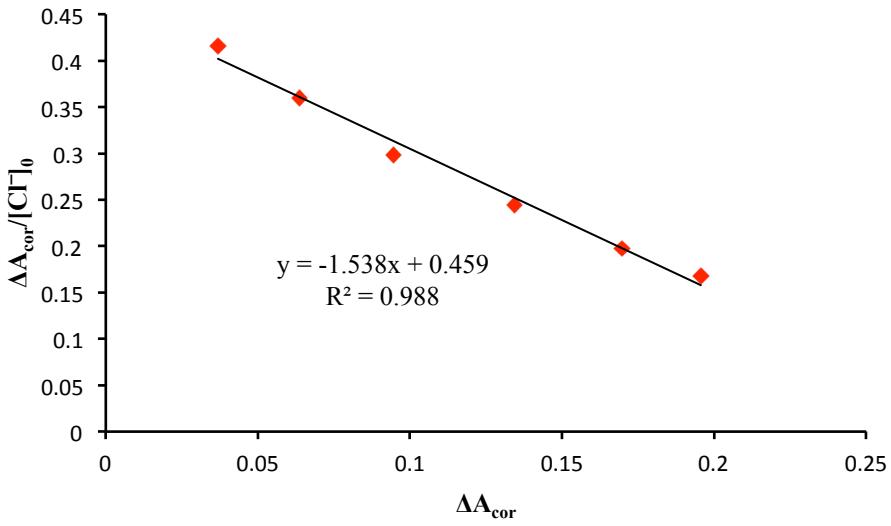

Figure S16. Linear least squares fitting of the titration data in Table S14.

Binding of 1-bis with $H_2PO_4^-$ in 25% (v/v) aqueous DMSO. A 22.5 μM solution of **1-bis** in 25% H_2O–DMSO (2.00 mL) was titrated with a 0.377 M solution of tetrabutylammonium dihydrogen phosphate in 25% H_2O–DMSO at 24 °C (Table S15). Non-linear curve fitting of the titration data affords $K = 28\ M^{-1}$ and $A_{max} = 0.169$ (Figure S17, 13-58% bound (i.e., $\Delta A/\Delta A_{max}$)).

Table S15. Data for the titration of **1-bis** with $H_2PO_4^-$ in 25% H_2O–DMSO at 389 nm.

Entry	μL $H_2PO_4^-$ added	$[thiourea]_0$, μM	$[H_2PO_4^-]_0$, mM	Observed absorption	Calculated absorption[a]
0		22.5	0	0.3151	0.3151
1	30	22.4	5.56	0.3349	0.3327
2	45	22.4	8.28	0.3400	0.3391
3	60	22.4	11.0	0.3446	0.3442
4	80	22.2	14.5	0.3493	0.3496
5	100	22.1	17.9	0.3515	0.3536
6	150	22.0	26.3	0.3582	0.3594
7	200	21.8	34.2	0.3622	0.3613
8	300	21.6	49.1	0.3594	0.3588

[a] From the non-linear curve fit.

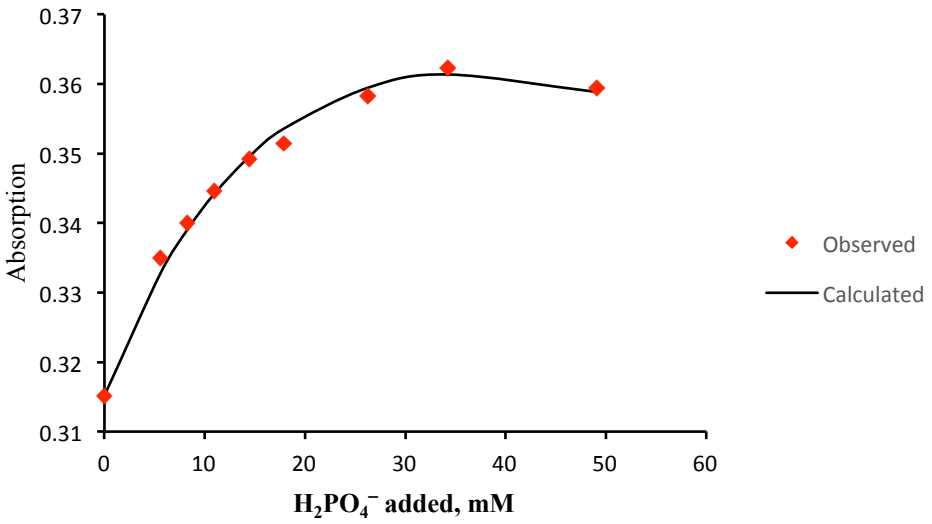

Figure S17. Non-linear least squares fitting of the titration data in Table S15.

Binding of 1-mono with $H_2PO_4^-$ in 25% (v/v) aqueous DMSO. A 45 μM solution of **1-mono** in 25% H_2O–DMSO (2.00 mL) was titrated with a 0.367 M solution of tetrabutylammonium dihydrogen phosphate in 25% H_2O–DMSO at 23 °C (Table S16). A linear least squares fit in the single-reciprocal plot affords K = 12 M^{-1} and ΔA_{max} = 0.315 (Figure S18, 4-54% bound (i.e., $\Delta A/\Delta A_{max}$)).

Table S16. Data for the titration of **1-mono** with $H_2PO_4^-$ in 25% H_2O–DMSO at 388 nm.

Entry	μL $H_2PO_4^-$ added	$[H_2PO_4^-]_0$, M	Observed absorption	ΔA_{cor}	$\Delta A_{cor}/ [H_2PO_4^-]_0$
0	0	0	0.3935	–	–
1	30	0.00542	0.4069	0.0194	3.582
2	60	0.01067	0.4173	0.0363	3.401
3	90	0.01578	0.4212	0.0465	2.949
4	140	0.02398	0.4307	0.0672	2.804
5	200	0.03332	0.4369	0.0870	2.612
6	300	0.04781	0.4393	0.1116	2.334
7	400	0.06109	0.4360	0.1295	2.119
8	500	0.07331	0.4315	0.1457	1.988
9	700	0.09504	0.4180	0.1706	1.795

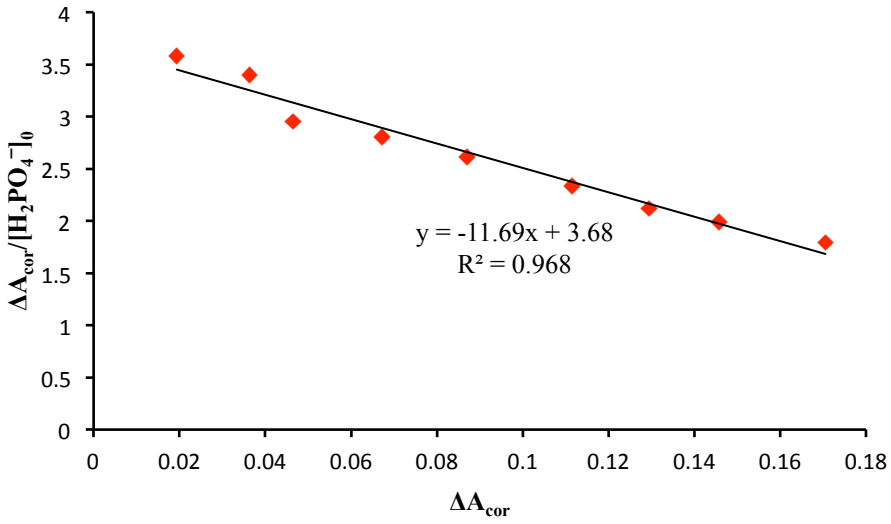

Figure S18. Linear least squares fitting of the titration data in Table S16.

Binding of 1-mono with OAc^- in 25% (v/v) aqueous DMSO. A 60 μM solution of **1-mono** in 25% H_2O–DMSO (1.00 mL) was titrated with a 0.367 M solution of tetrabutylammonium acetate in 25% H_2O–DMSO at 23 °C (Table S17). A linear least squares fit in the single-reciprocal plot affords K = 12 M^{-1} and ΔA_{max} = 0.436 (Figure S19, 9-68% bound (i.e., $\Delta A/\Delta A_{max}$)).

Table S17. Data for the titration of **1-mono** with OAc^- in 25% H_2O–DMSO at 387 nm.

Entry	μL OAc^- added	$[OAc^-]_0$, M	Observed absorption	ΔA_{cor}	$\Delta A_{cor}/[OAc^-]_0$
0	0	0	0.5513	–	–
1	15	0.00777	0.5829	0.0403	5.182
2	30	0.01532	0.6014	0.0681	4.443
3	50	0.02505	0.6207	0.1003	4.005
4	75	0.03670	0.6387	0.1352	3.684
5	100	0.04782	0.6454	0.1585	3.315
6	125	0.05845	0.6499	0.1796	3.073
7	150	0.06862	0.6597	0.2072	3.019
8	200	0.08769	0.6472	0.2250	2.566
9	250	0.1052	0.6357	0.2429	2.309
10	300	0.1214	0.6211	0.2558	2.106
11	400	0.1504	0.6010	0.2897	1.927
12	450	0.1633	0.5856	0.2973	1.820

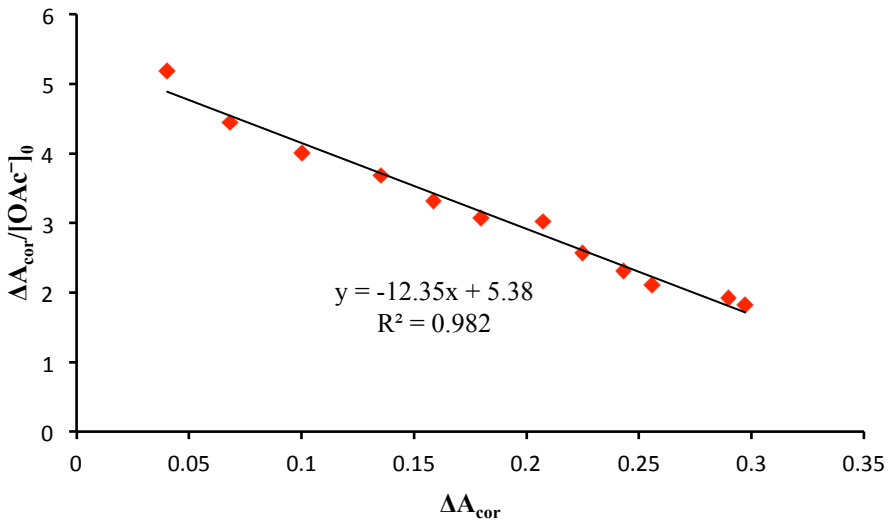

Figure S19. Linear least squares fitting of the titration data in Table S17.

Binding of 1-tris with $H_2PO_4^-$ in 30% (v/v) aqueous DMSO. A 15 μM solution of **1-tris** in 30% H_2O–DMSO (2.00 mL) was titrated with a 51.8 mM solution of tetrabutylammonium dihydrogen phosphate in 30% H_2O–DMSO at 23 °C (Table S18). Non-linear curve fitting of the titration data affords K = 1400 M^{-1} and A_{max} = 0.462 (Figure S20).

Binding of 1-tris with OAc^- in 30% (v/v) aqueous DMSO. A 15 μM solution of **1-tris** in 30% H_2O–DMSO (2.00 mL) was titrated with a 0.462 M solution of tetrabutylammonium acetate in 30% H_2O–DMSO containing 15 μM of **1-tris** at 23 °C (Table S19). Non-linear curve fitting of the titration data with a fixed ΔA_{max} = 0.120 (i.e., as for the 25% H_2O–DMSO) affords K = 13 M^{-1} (entries 1–7, 1-40% bound (i.e., $\Delta A/\Delta A_{max}$); deviation was observed thereafter presumably due to sequential 1:2 binding, Figure S21).

Table S18. Data for the titration of **1-tris** with $H_2PO_4^-$ in 30% H_2O–DMSO at 395 nm.

Entry	µL $H_2PO_4^-$ added	$[thiourea]_0$, µM	$[H_2PO_4^-]_0$, µM	Observed absorption	Calculated absorption[a]
0	0	15.00	0	0.2271	0.2271
1	2	14.99	52	0.2494	0.2425
2	4	14.97	103	0.2616	0.2559
3	6	14.96	155	0.2710	0.2678
4	9	14.93	232	0.2865	0.2830
5	12	14.91	308	0.2980	0.2958
6	16	14.88	411	0.3088	0.3101
7	22	14.84	563	0.3249	0.3269
8	30	14.78	764	0.3388	0.3434
9	40	14.71	1014	0.3548	0.3579
10	50	14.63	1262	0.3658	0.3681
11	70	14.49	1749	0.3798	0.3809
12	90	14.35	2227	0.3877	0.3879
13	115	14.19	2813	0.3942	0.3923
14	140	14.02	3384	0.3978	0.3940

[a] From the non-linear curve fit.

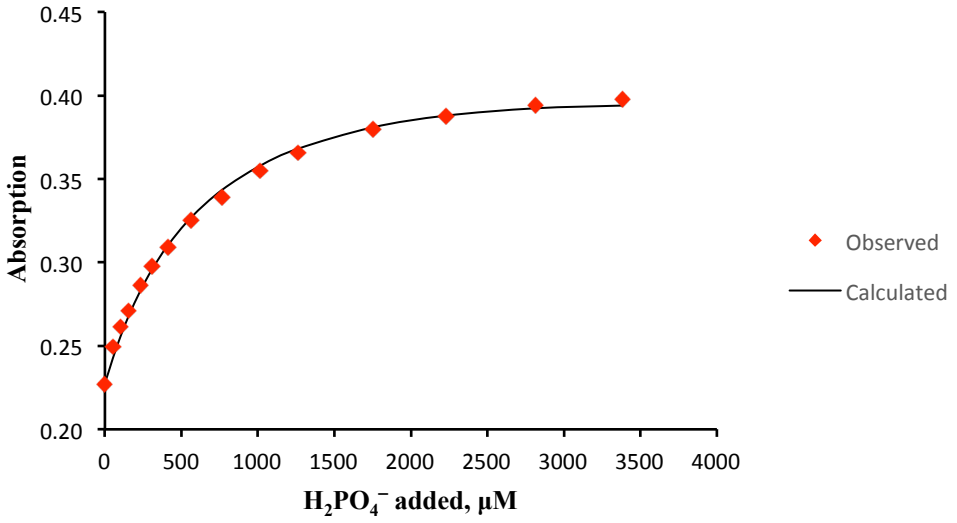

Figure S20. Non-linear least squares fitting of the titration data in Table S18.

Table S19. Data for the titration of **1-tris** with OAc^- in 30% H_2O–DMSO at 379 nm.

Entry	µL OAc^- added	$[thiourea]_0$, mM	$[OAc^-]_0$, mM	Observed absorption	Calculated absorption[a]
0	0	0.015	0.00	0.3736	0.3736
1	5	0.015	1.15	0.3742	0.3754
2	10	0.015	2.30	0.3749	0.3771
3	50	0.015	11.25	0.3868	0.3890
4	100	0.015	21.97	0.3975	0.4004
5	150	0.015	32.19	0.4088	0.4091
6	200	0.015	41.94	0.4167	0.4161
7	250	0.015	51.26	0.4249	0.4218
8	300	0.015	60.18	0.4372	0.4265
9	400	0.015	76.90	0.4532	0.4338
10	500	0.015	92.29	0.4678	0.4393
11	600	0.015	106.49	0.4751	0.4435
12	775	0.015	128.89	0.4904	0.4490

[a] From the non-linear curve fit.

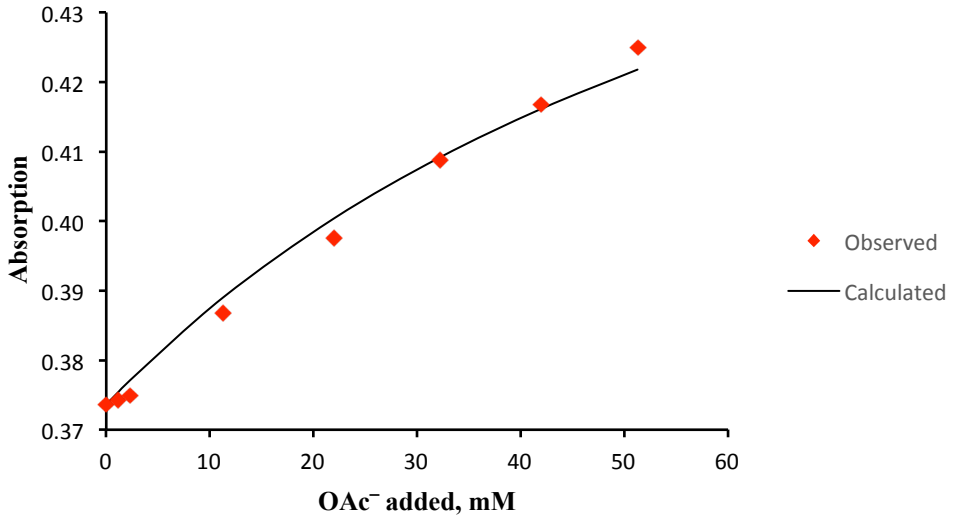

Figure S21. Non-linear least squares fitting of the titration data in Table S19.

Table S20. ^{31}P NMR chemical shifts of phosphorous compounds in presence and absence of **4-tris**.[a]

Entry	Phosphate compound	δ, ppm
1	$Bu_4N^+H_2PO_4^-$ • **4-tris**	0.5 ppm
2	$Bu_4N^+H_2PO_4^-$	2.2 ppm
3	$(Bu_4N^+)_2HPO_4^{2-}$	3.2 ppm
4	Extraction simulation[b]	4.1 ppm
5	$(Bu_4N^+)_2HPO_4^{2-}$ • **4-tris**	4.5 ppm

[a] Spectra taken of 10 mM solutions in $CDCl_3$. Dibasic phosphate was prepared by adding 1 equivalent of a 1.07 M $Bu_4N^+OH^-$ solution in methanol. [b] Employed conditions: 10 mM **4-tris** and 5.9 mM $(Bu_4N^+)_2HPO_4^{2-}$ in $CDCl_3$.

Figure 22. NMR spectra of **5**, **1-tris**, **1-bis** and **4-tris**.

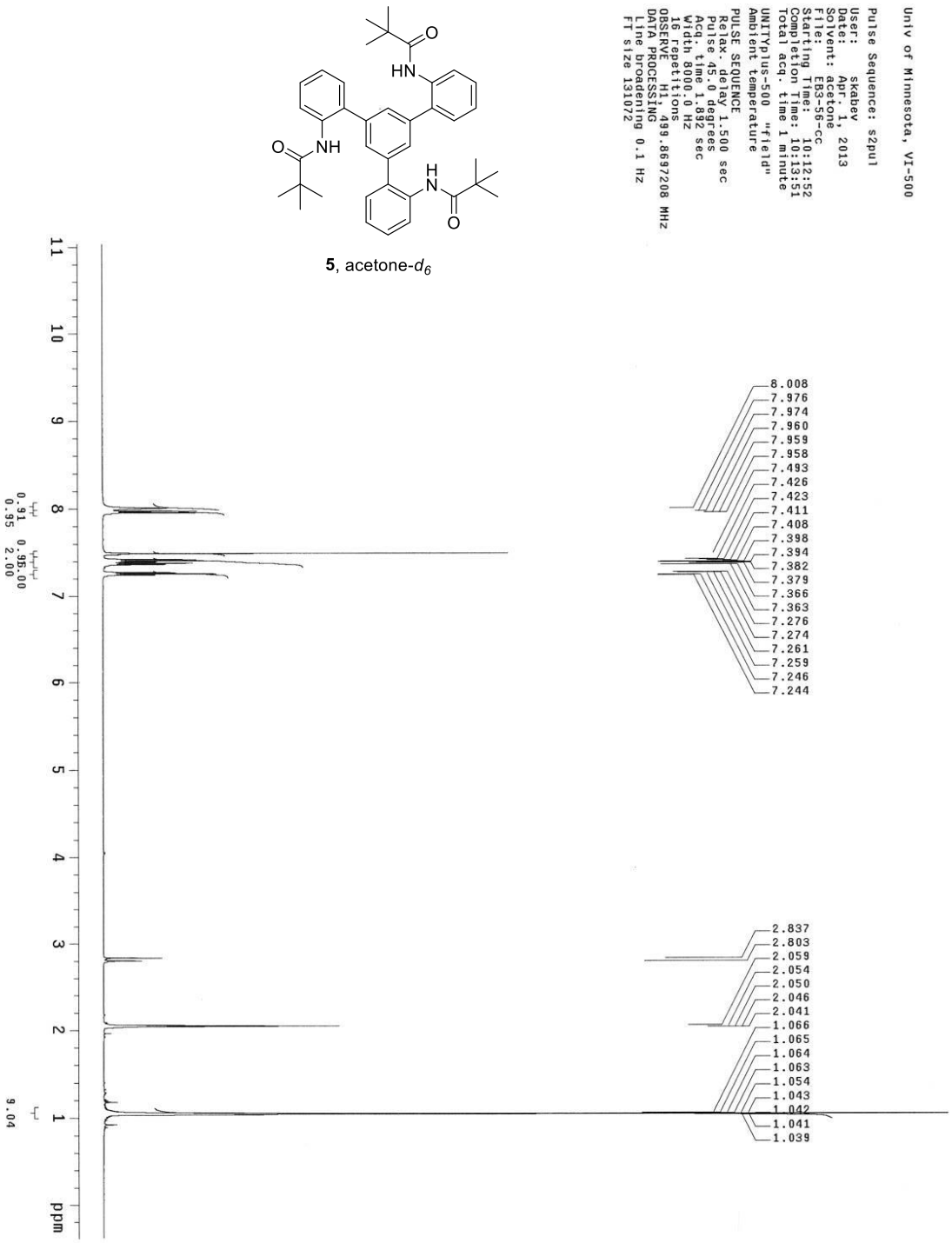

5, acetone-d_6

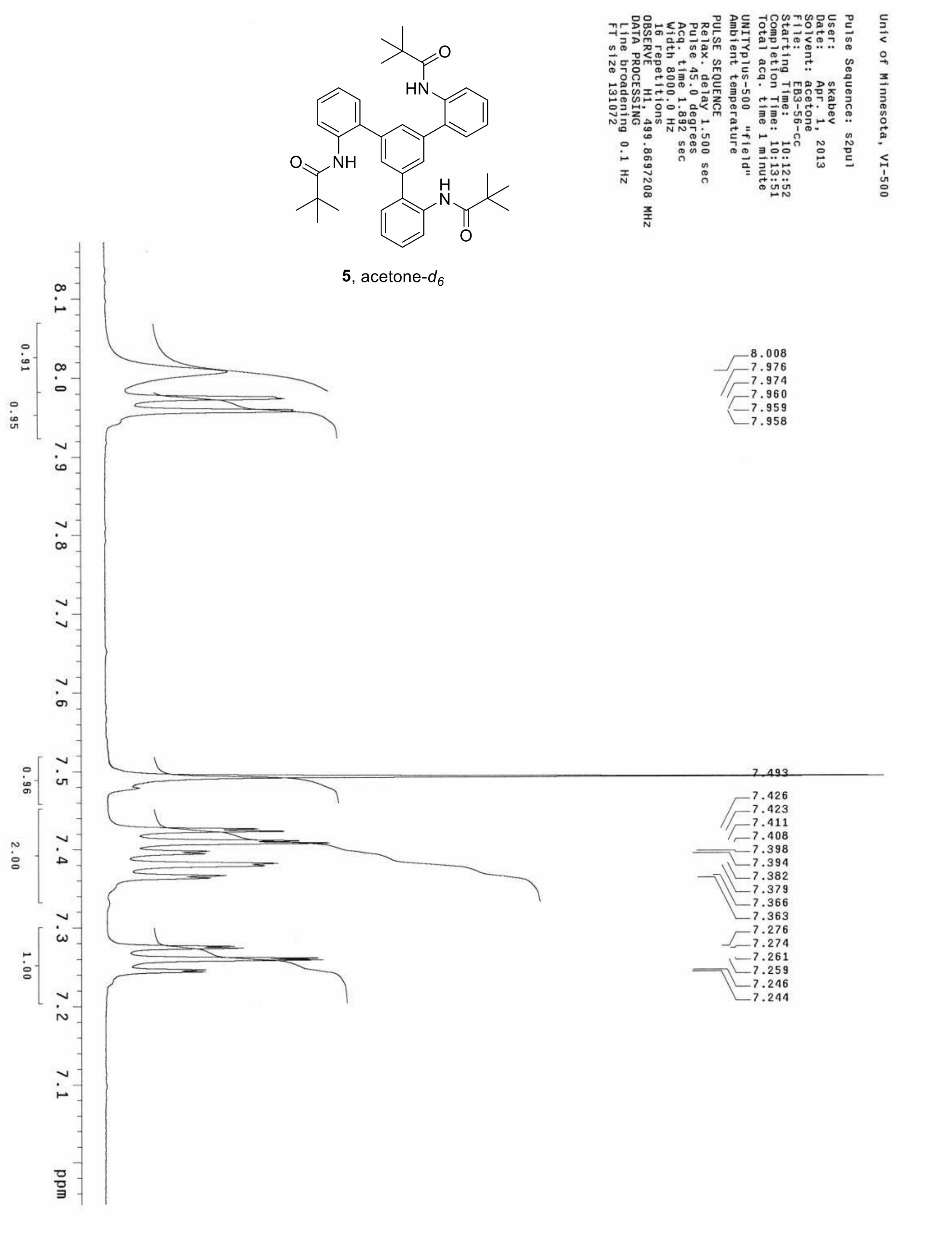
Univ of Minnesota, VI-500
Pulse Sequence: s2pul
User: skabev
Date: Apr. 1, 2013
Solvent: acetone
File: EB3-56-cc
Starting Time: 10:12:52
Completion Time: 10:13:51
Total acq. time 1 minute
UNITYplus-500 "field"
Ambient temperature
PULSE SEQUENCE
Relax. delay 1.500 sec
Pulse 45.0 degrees
Acq. time 1.892 sec
Width 8000.0 Hz
16 repetitions
OBSERVE H1, 499.8697208 MHz
DATA PROCESSING
Line broadening 0.1 Hz
FT size 131072
8.008
7.976
7.974
7.960
7.959
7.958
7.493
7.426
7.423
7.411
7.408
7.398
7.394
7.382
7.379
7.366
7.363
7.276
7.274
7.261
7.259
7.246
7.244
0.91
0.95
0.96
2.00
1.00
8.1
8.0
7.9
7.8
7.7
7.6
7.5
7.4
7.3
7.2
7.1
ppm

5, acetone-d_6

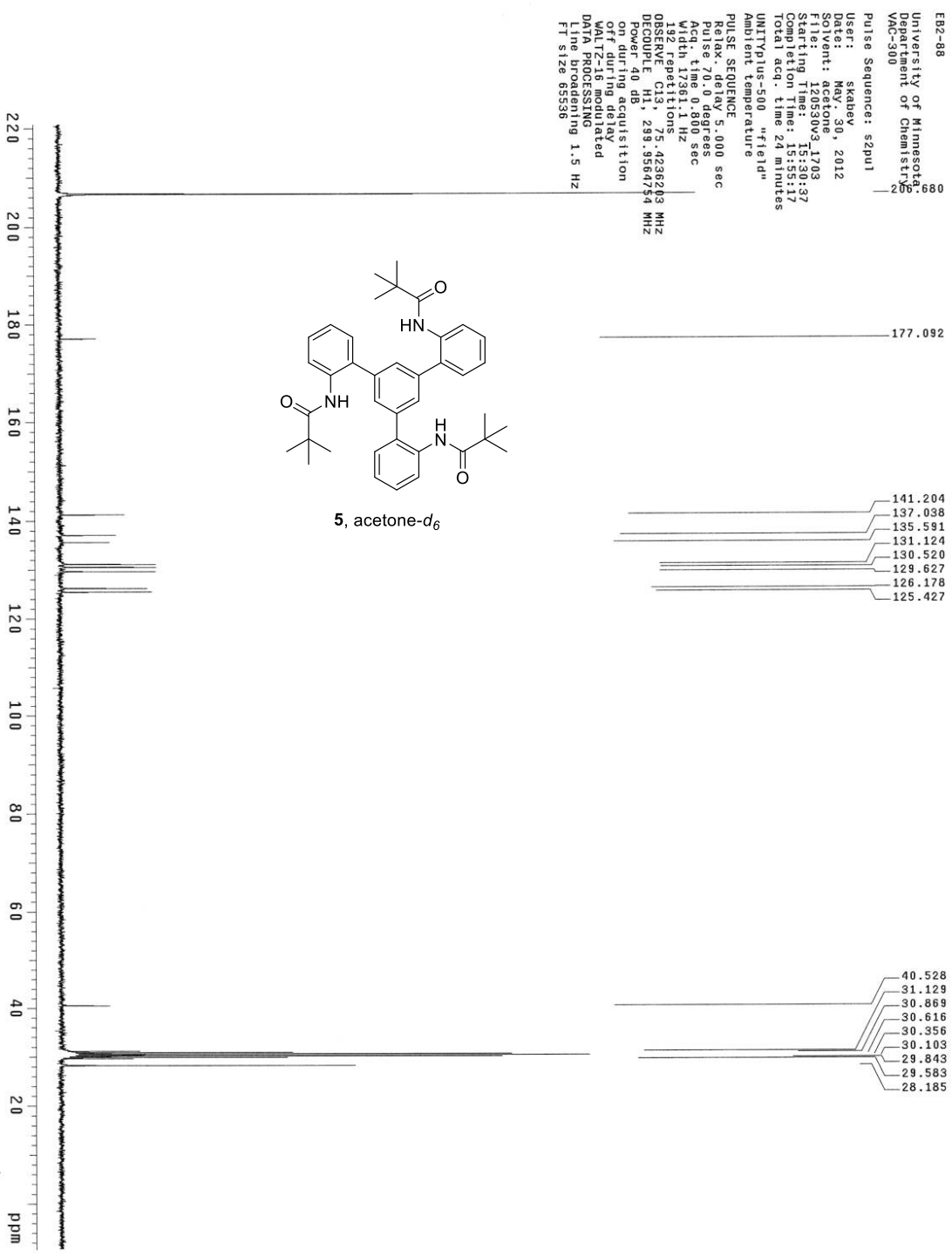
EB2-88
University of Minnesota
Department of Chemistry
VAC-300
Pulse Sequence: s2pul
User: skabey
Date: May 30, 2012
Solvent: acetone
File: 120530v3.1703
Starting Time: 15:30:37
Completion Time: 15:55:17
Total acq. time 24 minutes
UNITYplus-500 "field"
Ambient temperature
PULSE SEQUENCE
Relax. delay 5.000 sec
Pulse 70.0 degrees
Acq. time 0.800 sec
Width 17361.1 Hz
192 repetitions
OBSERVE C13, 75.4236203 MHz
DECOUPLE H1, 299.9564754 MHz
Power 40 dB
on during acquisition
off during delay
WALTZ-16 modulated
DATA PROCESSING
Line broadening 1.5 Hz
FT size 65536
206.680
177.092
141.204
137.038
135.591
131.124
130.520
129.627
126.178
125.427
40.528
31.129
30.869
30.616
30.356
30.103
29.843
29.583
28.185
220
200
180
160
140
120
100
80
60
40
20
ppm

5, acetone-d_6

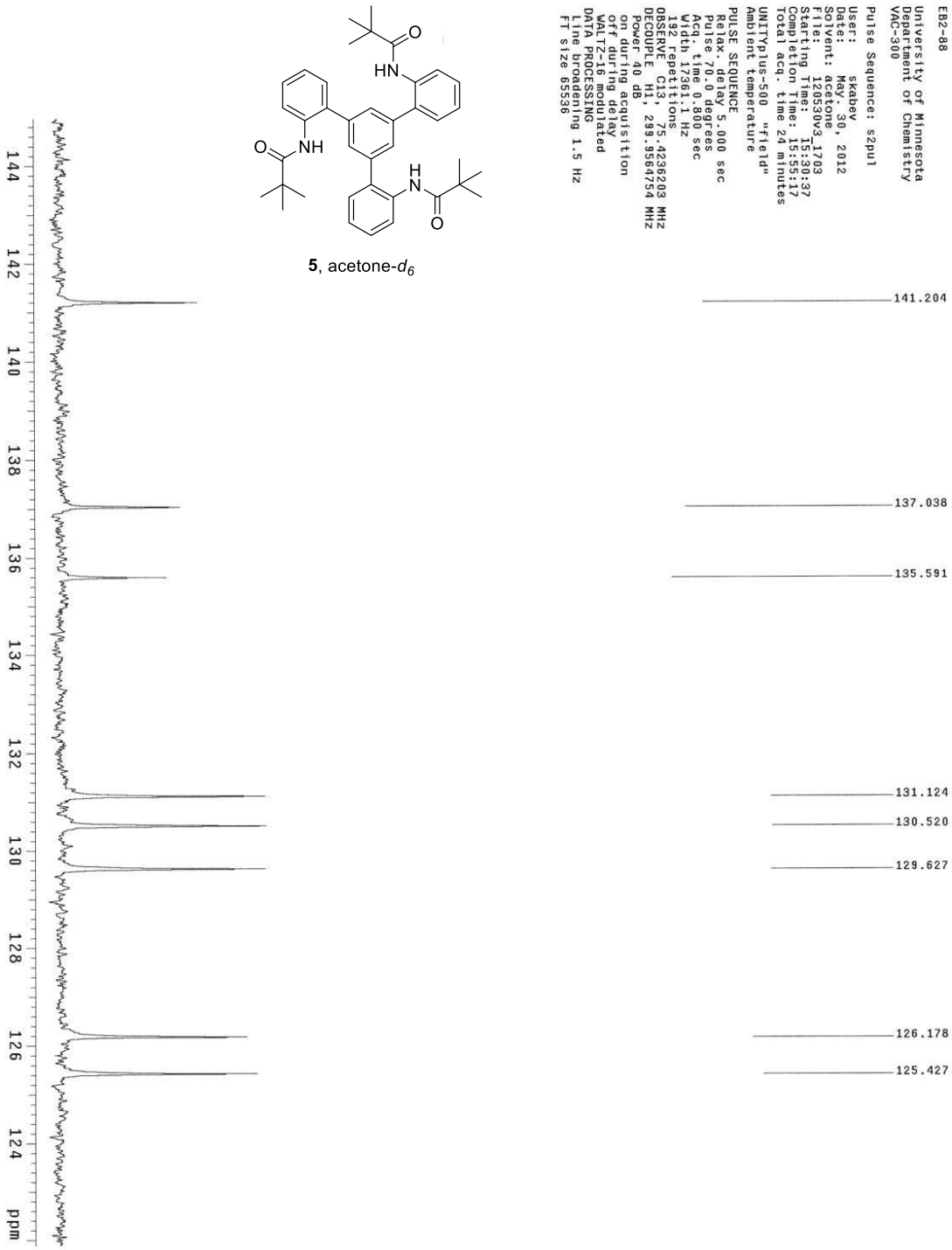
EB2-88
University of Minnesota
Department of Chemistry
VAC-300
Pulse Sequence: s2pul
User: skabey
Date: May 30, 2012
Solvent: acetone
File: 120530v3_1703
Starting Time: 15:30:37
Completion Time: 15:55:17
Total acq. time 24 minutes
UNITYplus-500 "field"
Ambient temperature
PULSE SEQUENCE
Relax. delay 5.000 sec
Pulse 70.0 degrees
Acq. time 0.800 sec
Width 17361.1 Hz
192 repetitions
OBSERVE C13, 75.423203 MHz
DECOUPLE H1, 299.956754 MHz
Power 40 dB
on during acquisition
off during delay
WALTZ-16 modulated
DATA PROCESSING
Line broadening 1.5 Hz
FT size 65536
141.204
137.038
135.591
131.124
130.520
129.627
126.178
125.427
144
142
140
138
136
134
132
130
128
126
124
ppm

5, acetone-d_6

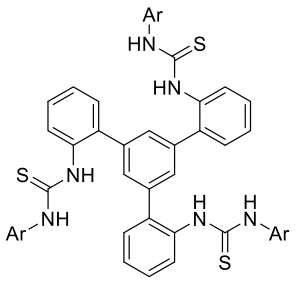

1-tris (Ar = *p*-$C_6H_4NO_2$), acetone-d_6

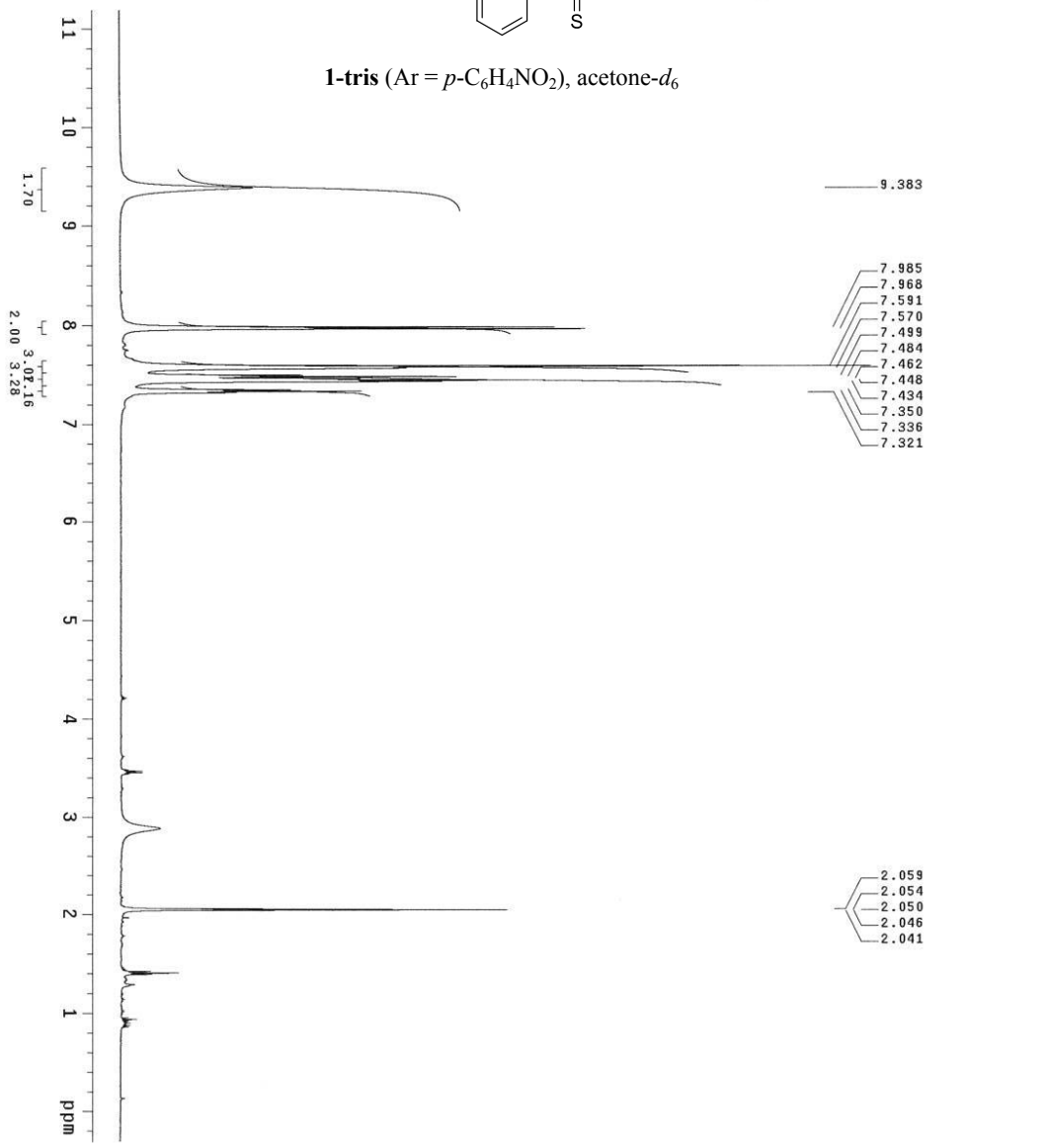

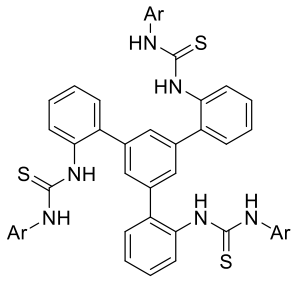

1-tris (Ar = *p*-$C_6H_4NO_2$), acetone-d_6

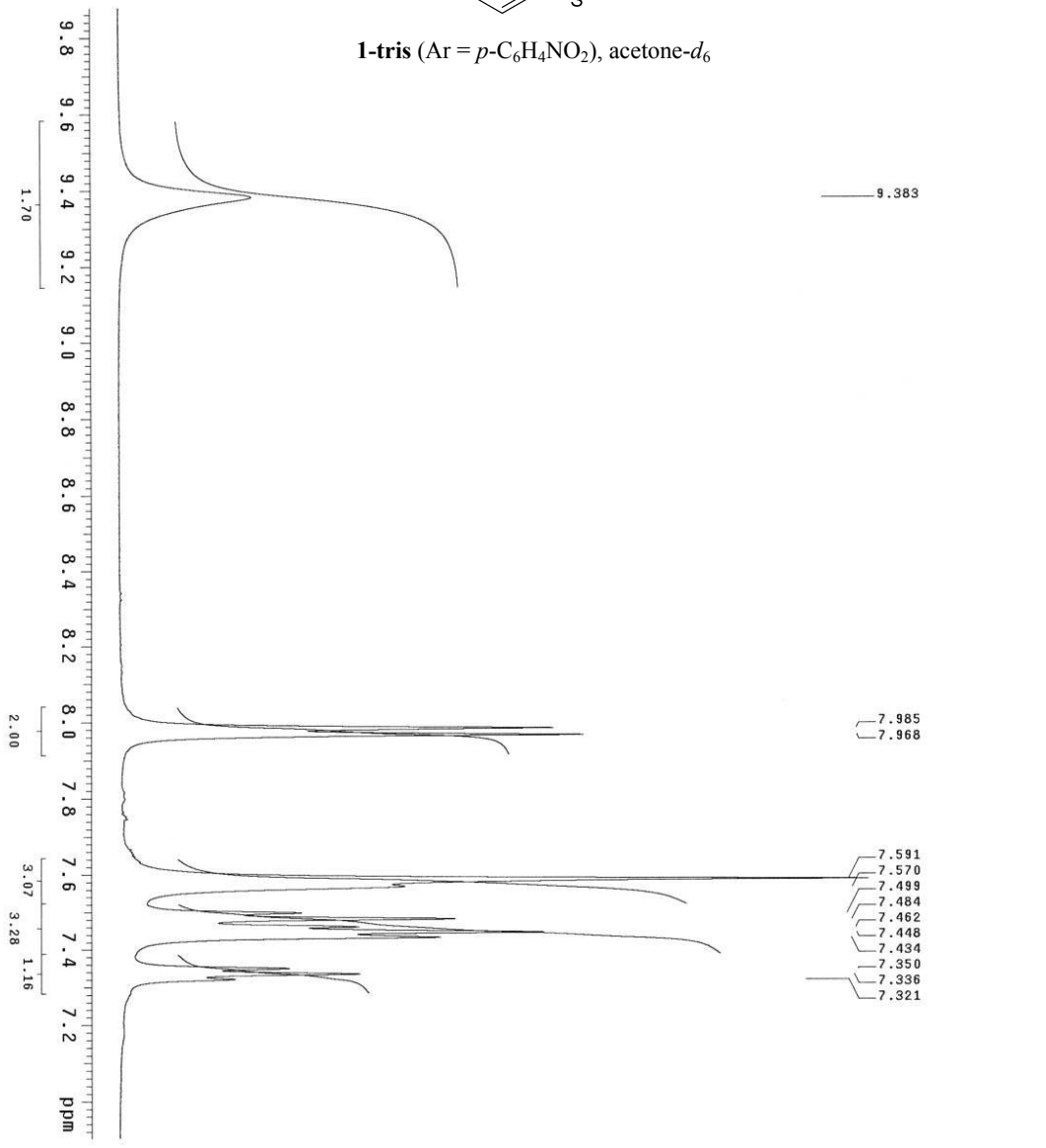

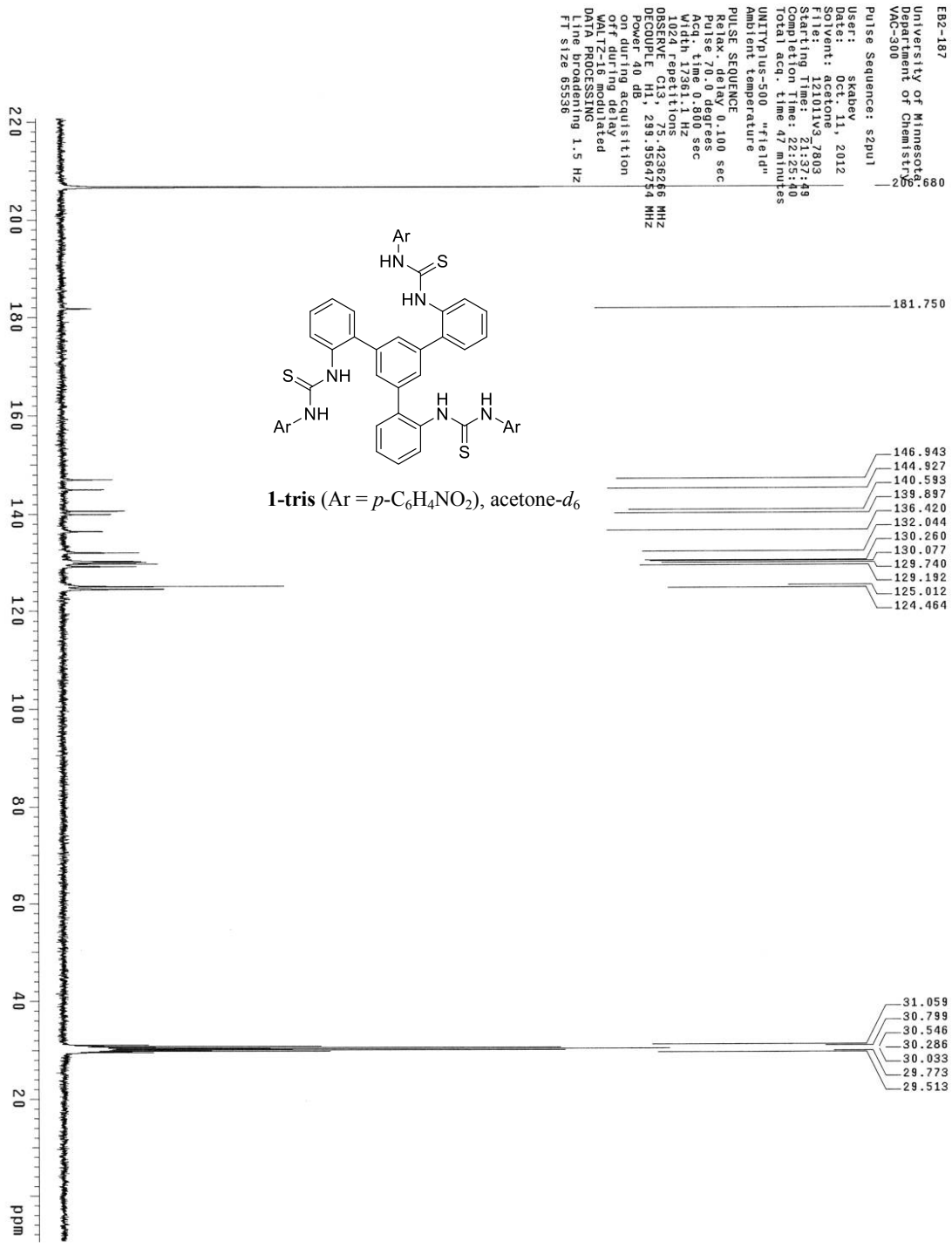

1-tris (Ar = *p*-$C_6H_4NO_2$), acetone-d_6

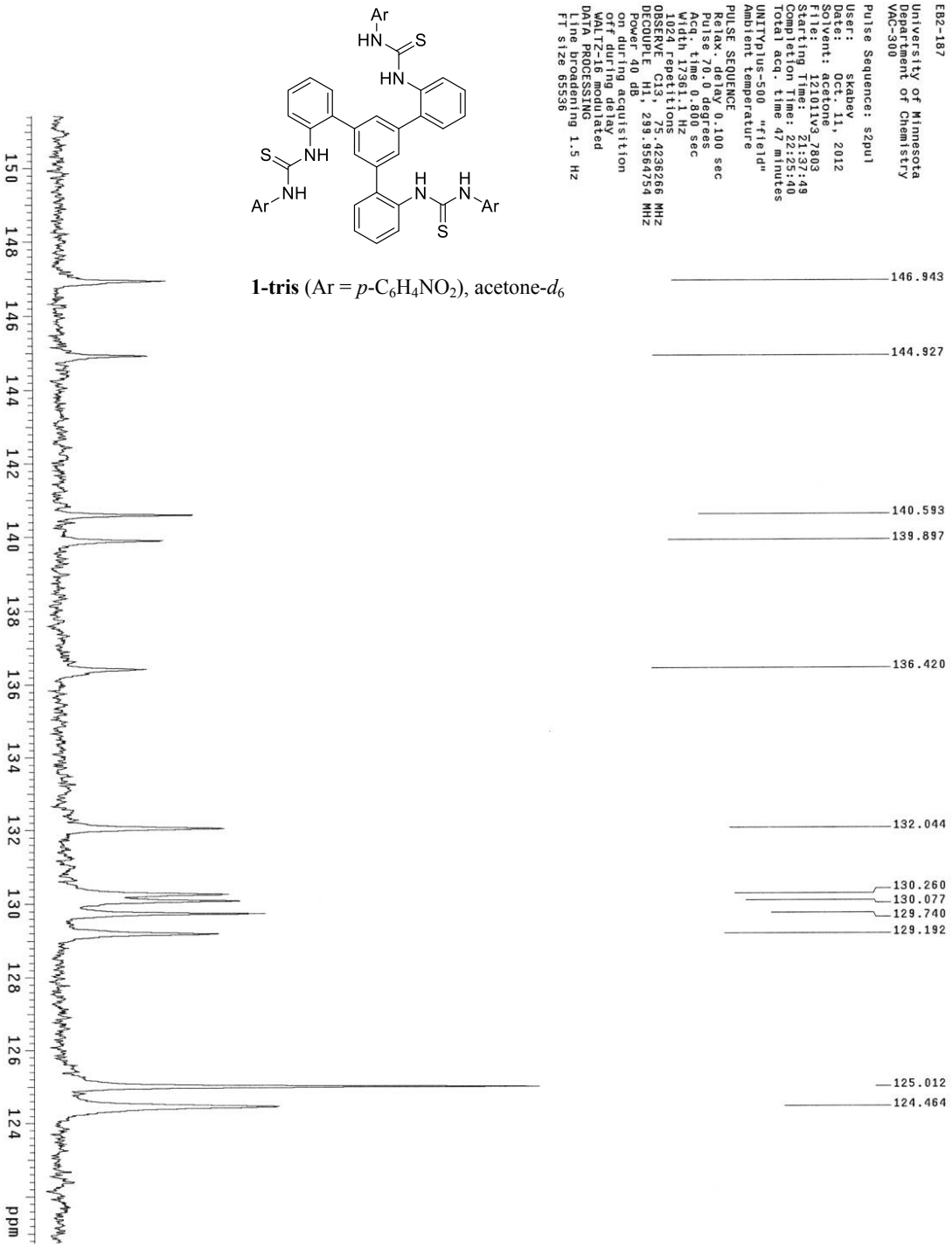

1-tris (Ar = *p*-$C_6H_4NO_2$), acetone-d_6

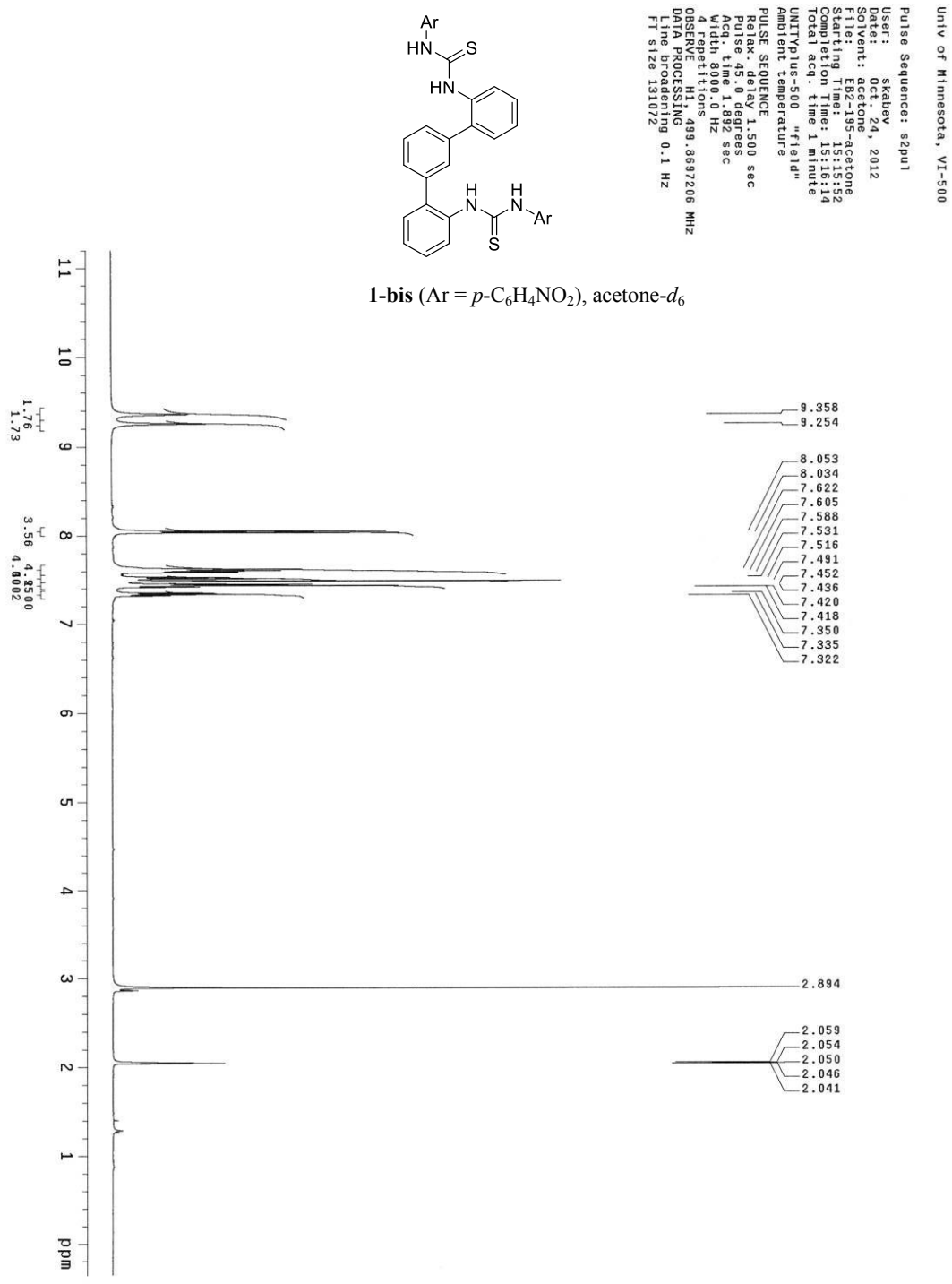

1-bis (Ar = *p*-$C_6H_4NO_2$), acetone-d_6

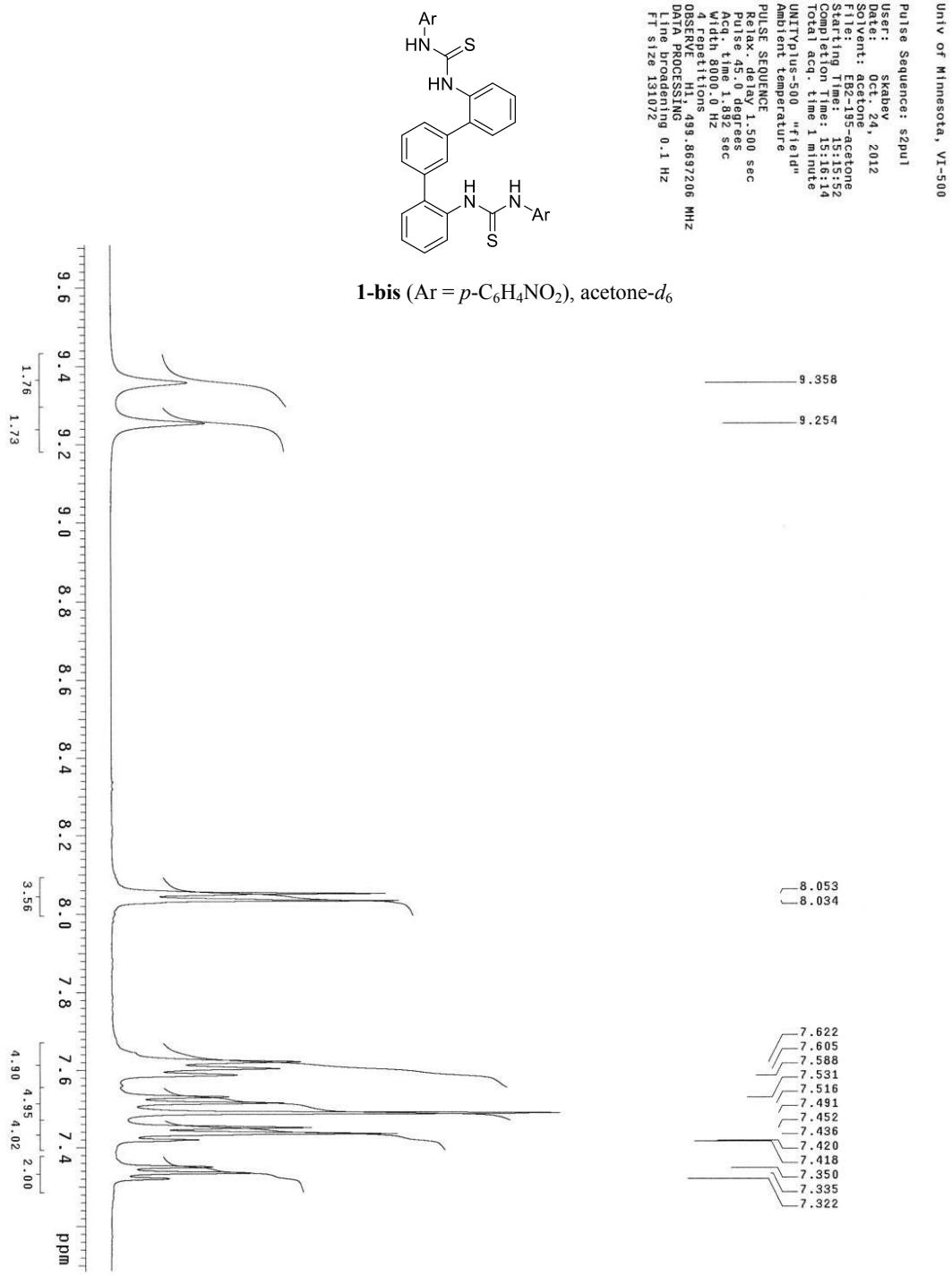

1-bis (Ar = *p*-$C_6H_4NO_2$), acetone-d_6

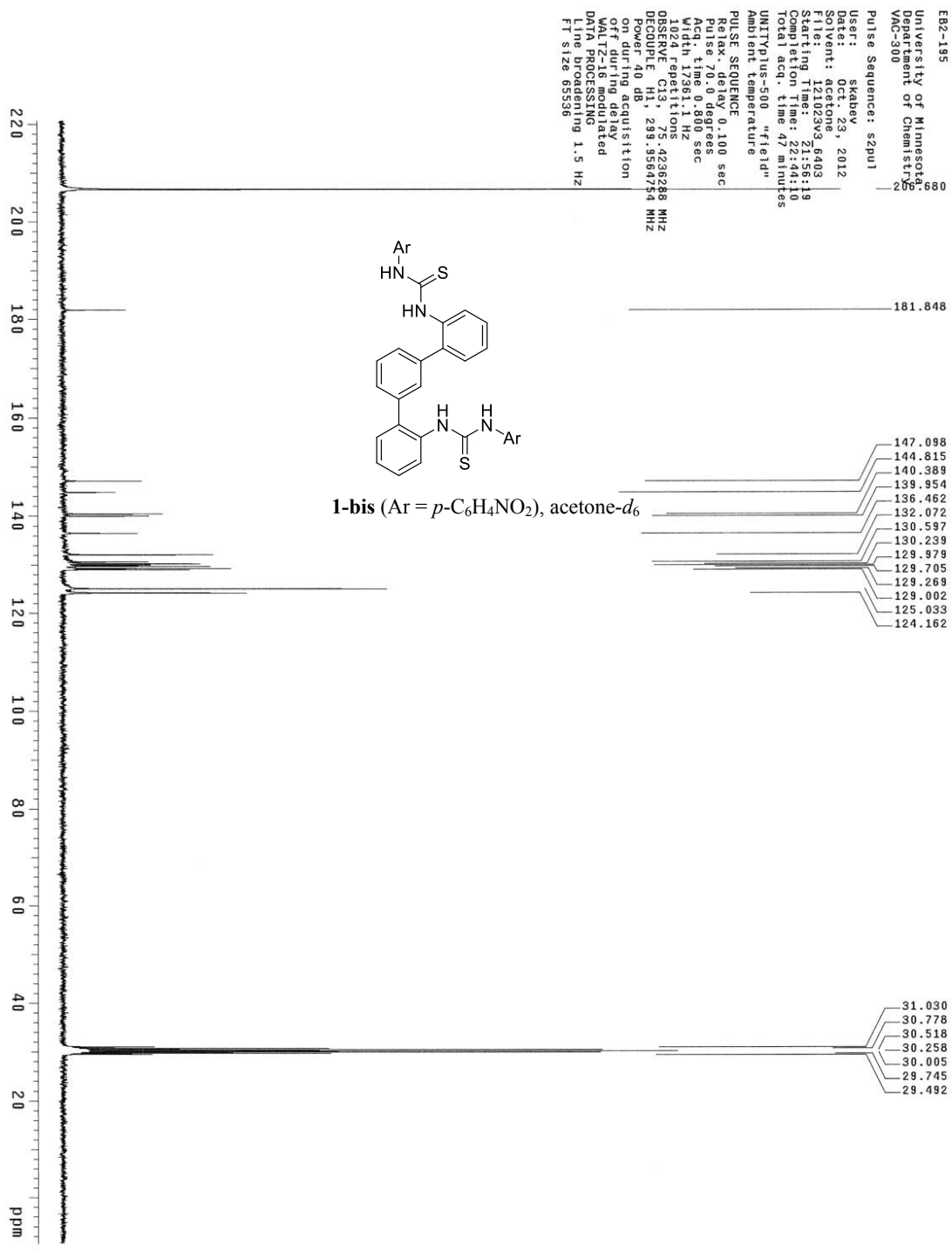

1-bis (Ar = *p*-$C_6H_4NO_2$), acetone-d_6

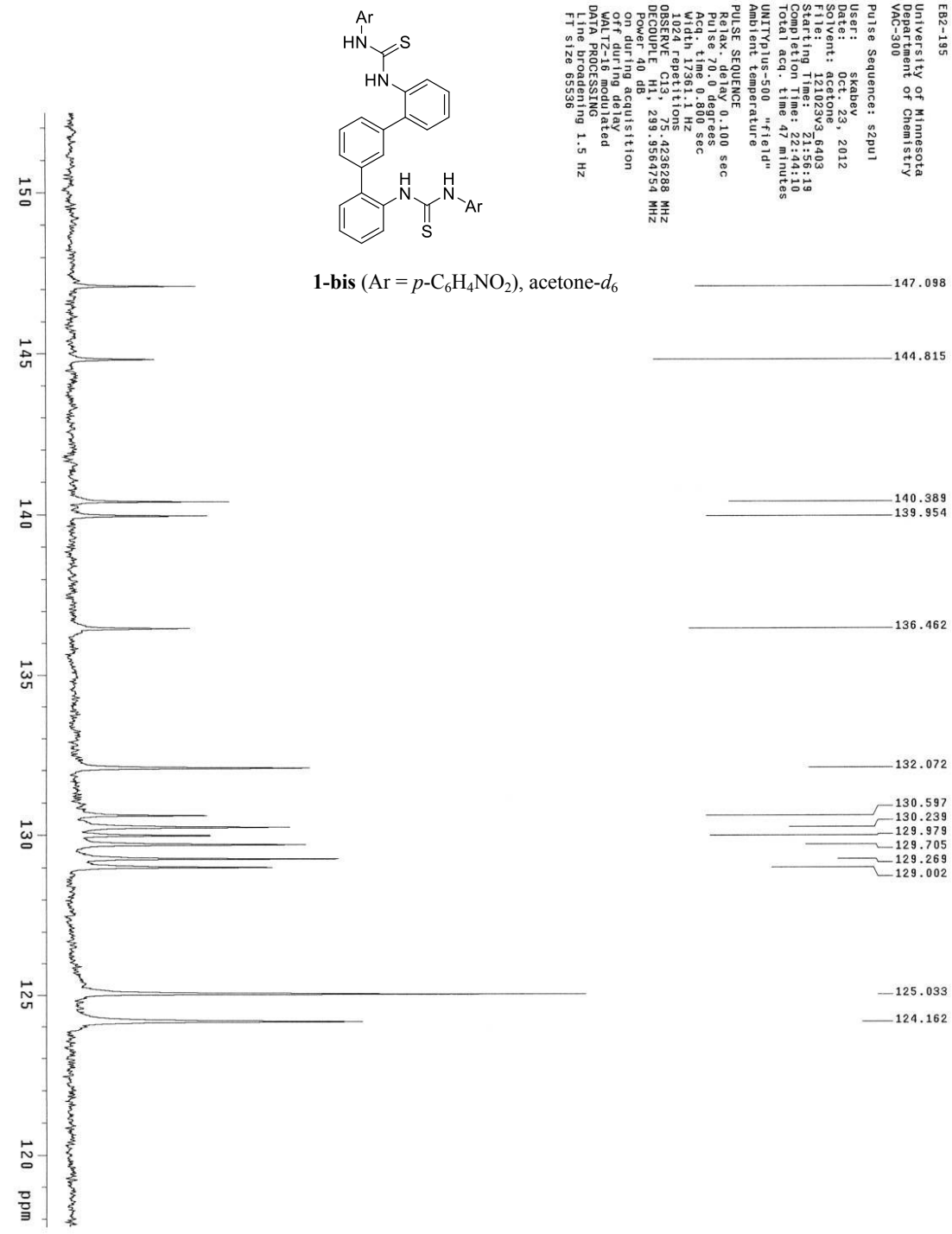

1-bis (Ar = *p*-$C_6H_4NO_2$), acetone-d_6

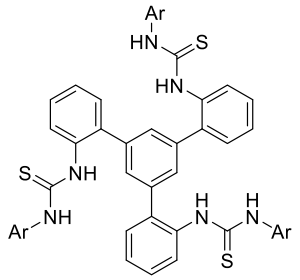

4-tris (Ar = 3,5-$(CF_3)_2C_6H_3$), $CDCl_3$

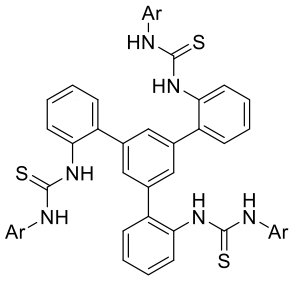

4-tris (Ar = 3,5-$(CF_3)_2C_6H_3$), $CDCl_3$

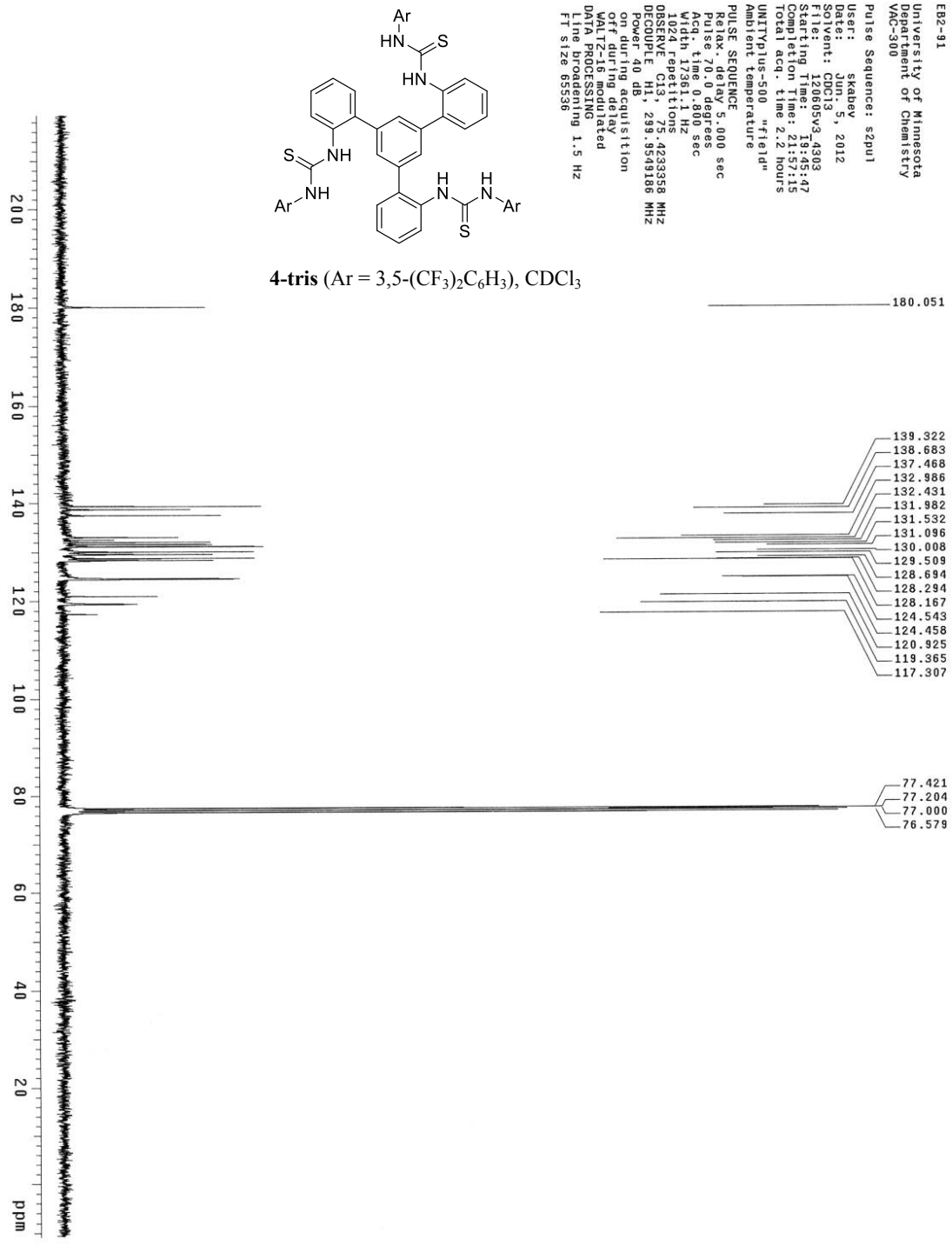

4-tris (Ar = 3,5-$(CF_3)_2C_6H_3$), $CDCl_3$

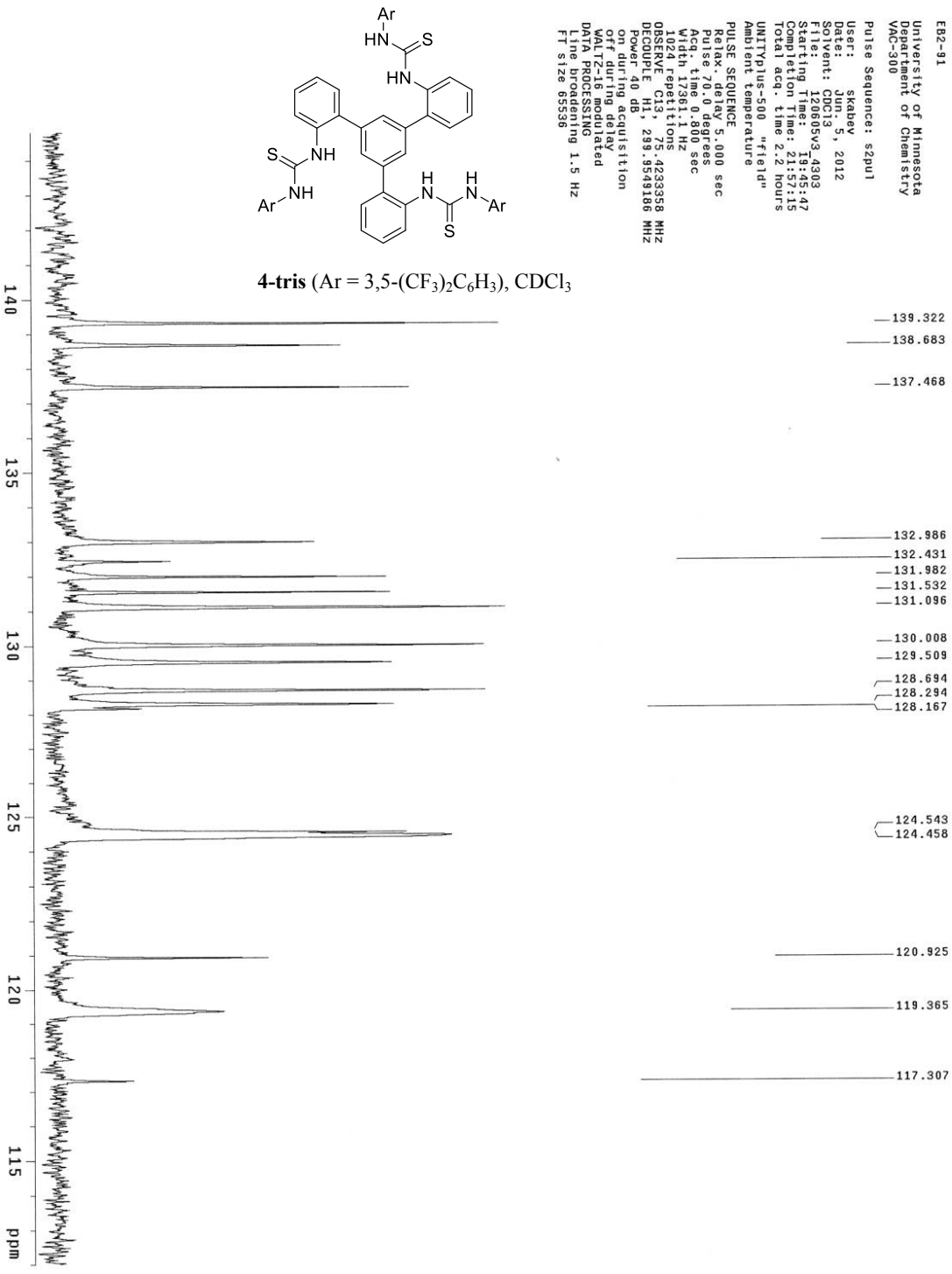

4-tris (Ar = 3,5-$(CF_3)_2C_6H_3$), $CDCl_3$

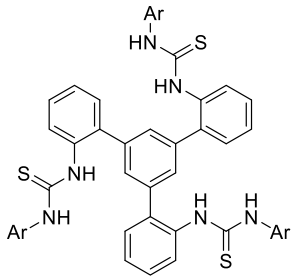

4-tris (Ar = 3,5-$(CF_3)_2C_6H_3$), $CDCl_3$

Table S21. Computed B3LYP/6-31+G(d,p) geometry for the structure provided in figure 3. Its electronic energy = -4517.031796 hartrees.

6	0	0.455629	-1.265082	3.045544
6	0	-0.941707	-1.227982	2.917632
6	0	-1.583710	0.017644	2.889201
6	0	-0.851127	1.214690	2.958252
6	0	0.547525	1.147682	3.043563
6	0	1.209886	-0.087986	3.090207
1	0	0.965049	-2.222723	3.081938
1	0	-2.664482	0.058436	2.801167
1	0	1.129437	2.064313	3.066546
6	0	-1.730810	-2.484898	2.783432
6	0	-1.392923	-3.479538	1.834582
6	0	-2.865804	-2.688384	3.585466
6	0	-2.184049	-4.628984	1.710522
6	0	-3.638695	-3.842248	3.474736
1	0	-3.127361	-1.929242	4.316563
6	0	-3.293035	-4.814380	2.532749
1	0	-1.925959	-5.368604	0.964360
1	0	-4.506125	-3.977808	4.113865
1	0	-3.893767	-5.712575	2.424016
6	0	-1.535821	2.539440	2.966780
6	0	-1.172138	3.491255	3.937272
6	0	-2.540958	2.888223	2.037602
6	0	-1.791363	4.736871	4.005921
1	0	-0.405904	3.228817	4.660557
6	0	-3.154893	4.145839	2.102831
6	0	-2.791339	5.062955	3.085072
1	0	-1.497394	5.446536	4.773874
1	0	-3.914176	4.394337	1.371307
1	0	-3.279614	6.032413	3.122822
7	0	-0.310865	-3.239687	0.943563
1	0	-0.186655	-2.263275	0.680371
7	0	2.945281	1.062294	1.057409
1	0	2.221726	0.534729	0.556501
7	0	-2.851532	2.000531	0.971260
1	0	-2.052552	1.628351	0.451327
6	0	3.185928	2.355909	0.694077
6	0	0.707571	-4.086483	0.584974
6	0	-4.088085	1.530555	0.618688
16	0	4.062082	3.443619	1.628250
16	0	0.861852	-5.663843	1.139348
16	0	-5.487071	1.863046	1.493819
7	0	2.641254	2.650562	-0.544225
1	0	2.320165	1.861691	-1.102657
7	0	-3.995813	0.733923	-0.506450
1	0	-3.037384	0.622137	-0.856134
7	0	1.599362	-3.432356	-0.247699
1	0	1.424541	-2.424301	-0.356027
6	0	2.695537	-0.177283	3.162059
6	0	3.302875	-0.898299	4.205166
6	0	3.525192	0.407569	2.185305
6	0	4.687831	-1.019258	4.293925
1	0	2.668667	-1.351974	4.961287

6	0	4.916569	0.272750	2.267385
6	0	5.498425	-0.427821	3.320278
1	0	5.131778	-1.573450	5.115795
1	0	5.533159	0.722780	1.497718
1	0	6.579099	-0.521214	3.372820
8	0	-1.219329	0.752528	-1.065793
8	0	0.948704	-0.663785	-0.501373
15	0	-0.008185	-0.030635	-1.498715
8	0	-0.550875	-1.160142	-2.550618
1	0	0.137265	-1.790143	-2.808750
8	0	0.957110	0.945923	-2.422171
1	0	0.414526	1.593184	-2.897931
6	0	2.726567	-3.864193	-0.945186
6	0	3.522772	-2.839965	-1.515296
6	0	3.097347	-5.208595	-1.157824
6	0	4.648194	-3.140508	-2.263935
1	0	3.243948	-1.803233	-1.354069
6	0	4.227427	-5.508181	-1.909386
1	0	2.504265	-6.000532	-0.725805
6	0	4.999212	-4.481094	-2.457457
1	0	5.259393	-2.356832	-2.694058
1	0	4.515830	-6.538473	-2.078248
6	0	2.540470	3.877674	-1.210741
6	0	2.578940	3.846761	-2.620946
6	0	2.344663	5.110004	-0.558271
6	0	2.435135	5.009710	-3.364905
1	0	2.745771	2.900809	-3.126489
6	0	2.204992	6.276245	-1.299754
1	0	2.305215	5.146024	0.520606
6	0	2.253699	6.222402	-2.695610
1	0	2.476475	4.993510	-4.446898
1	0	2.045900	7.227781	-0.807783
6	0	-4.934066	0.030140	-1.256691
6	0	-4.402113	-0.769125	-2.299845
6	0	-6.332645	0.067732	-1.075500
6	0	-5.231051	-1.500150	-3.132651
1	0	-3.326490	-0.812491	-2.444154
6	0	-7.162443	-0.667927	-1.913152
1	0	-6.749264	0.668652	-0.280962
6	0	-6.616373	-1.446273	-2.936457
1	0	-4.823485	-2.112283	-3.927453
1	0	-8.237123	-0.641252	-1.780669
7	0	-7.495014	-2.210000	-3.808396
8	0	-8.715450	-2.152641	-3.607723
8	0	-6.981917	-2.881952	-4.713089
7	0	2.112091	7.451658	-3.469275
8	0	1.974721	8.514939	-2.854287
8	0	2.136083	7.368968	-4.703177
7	0	6.181875	-4.806943	-3.241814
8	0	6.475177	-5.999844	-3.390156
8	0	6.836854	-3.874499	-3.724811

References

40. F. G. Bordwell and D. J. Algrim, *J. Am. Chem. Soc.*, 1988, **110**, 2964-2968.

41. G. Jakab, C. Tancon, Z. Zhan, K. Lippert and P. R. Schreiner, *Org. Lett.,* 2012, **14**, 1724-1727.

42. E. J. Olson and P. Buhlmann, *J. Org. Chem.*, 2011, **76**, 8406-8412.

43. For a related observation, see: P. A. Gale, J. R. Hiscock, S. J. Moore, C. Caltagirone, M. B. Hursthouse and M. E. Light, *Chem. Asian J.* 2010, **5**, 555-561.